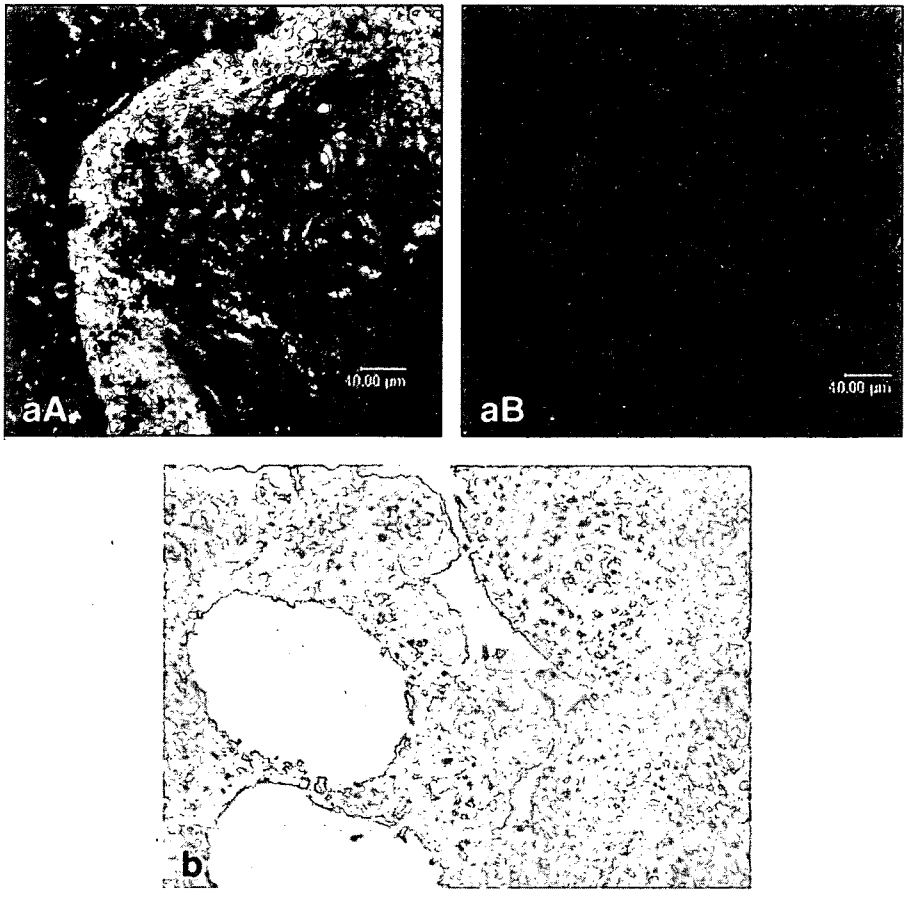

FIG. 7. Immunostaining of PADI4 and citrulline in OA synovial tissue. (a) Double immunofluorescent labelling shows CD68 macrophages (green in aA) and PADI4 signal (red in aB). Expression of PADI4 is relatively weak in macrophages of OA synovial tissue. Scale bar, 40 µm. (b) No significant immunosignals for citrullinated peptide in OA synovial tissues. Original magnification, 100×.

whereas the PADI4 protein level remains unchanged [19]. Because PADI4 transcripts with single-nucleotide polymorphisms conferring RA susceptibility have a longer half-life than non-susceptible mRNA [14], we postulate that mRNA with an RA susceptible-haplotype accumulates and becomes translated into more protein products in the RA inflamed synovium. Therefore, the high abundance of PADI4 in the synovial membrane is a prominent feature of RA pathogenesis.

Excessive fibrin formation is a prominent event of the inflamed RA joint [5, 23–25]. Amorphous fibrin deposits have been detected in the lining and deep layer of RA synovial membrane [23]. Based on our observations, fibrin aggregates appeared in the RA synovium as a solid block or as a loose tissue structure, and both forms were considerably citrullinated. However, only the loose fibrin structure expressed intracellular and extracellular PADI4. In these structures, PADI4-positive cells co-located with protein that contained citrulline, apoptotic cells that contained fragmented DNA and CK18 cleaved by caspase. Furthermore, most apoptotic cells of the RA synovium were localized in the spongiform fibrin mass. The co-localization of PADI4 and apoptotic cells in citrullinated fibrin with a loose tissue structure supports the notion that PADI4 plays a role in apoptosis and locally citrullinates fibrin, possibly by initiating apoptosis as described by Vossenaar *et al.* [19]. Then, the enzyme might leak from dead cells and continually catalyse extracellular fibrin protein. As a result, the spongy fibrin develops into a solid block after citrullination and the PADI4 enzyme is degraded extracellularly. This could explain why PADI4 expression was essentially undetectable in the solid fibrin block. In the rabbit model of antigen-induced arthritis, Sanchez-Pernaute *et al.* observed meshed fibrin at the initial stage of joint inflammation. They postulated that citrullination facilitates proteolytic fibrin cleavage and that fibrin after structural transformation activates the autoimmune reaction of RA [5, 25].

In most of the RA synovial tissue samples we tested, an antibody against IgA rather than other immunoglobulins recognized citrullinated fibrin, although some fibrin clots were also mildly immunostained with anti-IgM antibody. The IgA autoantibody has been broadly identified in rheumatoid disease. Among diverse types of RF, IgA RF is more frequently detected than IgM RF or IgG RF in the sera of individuals before a diagnosis of RA [26]. Berthelot *et al.* found the IgA class of APF in RA sera, though IgA APF was less sensitive than its classical IgG isotype [27]. Therefore, RA patients might develop an IgA class of anti-citrullinated protein antibody in response to a high concentration of citrullinated fibrin protein in the synovium. In fact, Masson-Bessiere *et al.* have reported that some fibrin in the RA synovial membrane is citrullinated and that the α and β chains of fibrin are the major targets of AFA [23]. The present study supports the notion that citrullinated fibrin triggers citrulline-specific B-cell maturation and thereby leads to RA autoimmunity [5, 23].

Although PADI4 was widely distributed in the lining and sublining of the RA synovial membrane, only a few cells of the

tissue expressed citrullinated protein. Baeten *et al.* obtained similar results using two commercially available anti-citrulline antibodies (Upstate and Biogenesis) [28]. This observation implies that the PADI4 enzyme is inactive in most RA synovial cells as well as in peripheral blood. The activation of PADI requires a high concentration of Ca^{2+} (10^{-5} mol/l) [29]. Under normal physiological conditions, the cytosolic and nucleoplasmic Ca^{2+} concentration of 10^{-7} mol/l is too low to trigger PADI enzymatic activity [19, 29]. Vossenaar *et al.* recently found that a high concentration of calcium ions induced by ionomycin could stimulate PADI and the subsequent citrullination of intracellular protein in RA synovial macrophages [19]. Ionomycin is a calcium ionophore that facilitates a sustained Ca^{2+} influx [30]. Thus, an altered level of calcium ions should explain the disparate expression of PADI4 enzyme and citrullinated peptides. However, exactly how Ca^{2+} leads to apoptosis involving PADI4 and subsequent fibrin citrullination remains unknown.

In summary, we demonstrated extensive PADI4 expression in diverse leucocyte subtypes of RA synovial tissue. We also observed significant citrullination of fibrin, as well as the co-location of PADI4, citrullinated protein and apoptosis in some fibrin deposits of the tissue. These findings might be helpful in understanding the close association of the PADI4 haplotype with RA and the important role of PADI4 in RA pathogenesis.

The authors have declared no conflicts of interest.

References

1. Corrigall VM, Panayi GS. Autoantigens and immune pathways in rheumatoid arthritis. Crit Rev Immunol 2002;22:281–93.
2. Vincent C, de Keyser F, Masson-Bessiere C, Sebbag M, Veys EM, Serre G. Anti-perinuclear factor compared with the so called antikeratin antibodies and antibodies to human epidermis filaggrin, in the diagnosis of arthritis. Ann Rheum Dis 1999;58:42–8.
3. Vencovsky J, Machacek S, Sedova L *et al.* Autoantibodies can be prognostic markers of an erosive disease in early rheumatoid arthritis. Ann Rheum Dis 2003;62:427–30.
4. Bas S, Genevay S, Meyer O, Gabay C. Anti-cyclic citrullinated peptide antibodies, IgM and IgA rheumatoid factors in the diagnosis and prognosis of rheumatoid arthritis. Rheumatology 2003;42:677–80.
5. Sanchez-Pernaute O, Largo R, Calvo E, Alvarez-Soria MA, Egido J, Herrero-Beaumont G. A fibrin based model for rheumatoid synovitis. Ann Rheum Dis 2003;62:1135–8.
6. Schellekens GA, de Jong BA, van den Hoogen FH, van de Putte LB, van Venrooij WJ. Citrulline is an essential constituent of antigenic determinants recognized by rheumatoid arthritis-specific autoantibodies. J Clin Invest 1998;101:273–81.
7. Nakamura RM. Progress in the use of biochemical and biological markers for evaluation of rheumatoid arthritis. J Clin Lab 2000;14:305–13.
8. Schellekens GA *et al.* The diagnostic properties of rheumatoid arthritis antibodies recognizing a cyclic citrullinated peptide. Arthritis Rheum 2000;43:155–63.
9. Van Venrooij WJ, Pruijn, GJ. Citrullination: a small change for a protein with great consequences for rheumatoid arthritis. Arthritis Res 2000;2:249–51.
10. Tarcsa E *et al.* Protein unfolding by peptidylarginine deiminase. Substrate specificity and structural relationships of the natural substrates. J Biol Chem 1996;271:30709–16.
11. Cornelis F *et al.* New susceptibility locus for rheumatoid arthritis suggested by a genome-wide linkage study. Proc Natl Acad Sci USA 1998;95:10746–50.
12. Shiozawa S *et al.* Identification of the gene loci that predispose to rheumatoid arthritis. Int Immunol 1998;10:1891–95.
13. Vossenaar ER, Zendman AJW, van Venrooij WJ. Pruijn GZM. PAD, a growing family of citrullinating enzymes: genes, features and involvement in disease. Bioassay 2003;25:1106–18.
14. Suzuki A *et al.* Functional haplotypes of PADI4, encoding citrullinating enzyme peptidylarginine deiminase 4, are associated with rheumatoid arthritis. Nat Genet 2003;34:395–402.
15. Nakashima K, Hagiwara T, Ishigami A *et al.* Molecular characterization of peptidylarginine deiminase in HL-60 cells induced by retinoic acid and 1alpha, 25-dihydroxyvitamin D(3). J Biol Chem 1999;274: 27786–92.
16. Asaga H, Nakashima K, Senshu T, Ishigami A, Yamada M. Immunocytochemical localization of peptidylarginine deiminase in human eosinophils and neutrophils. J Leukoc Biol 2001;70:46–51.
17. Hagiwara T, Nakashima K, Hirano H, Senshu T, Yamada M. Deimination of arginine residues in nucleophosmin/B23 and histones in HL-60 granulocytes. Biochem Biophys Res Commun 2002;290:979–86.
18. Nakashima K, Hagiwara T, Yamada M. Nuclear localization of peptidylarginine deiminase V and histone deimination in granulocytes. J Biol Chem 2002;277:49562–8.
19. Vossenaar ER, Radstake TR, Van Der Heijden A *et al.* Expression and activity of citrullinating peptidylarginine deiminase enzymes in monocytes and macrophages. Ann Rheum Dis 2004;63:373–81.
20. Hacker G. The morphology of apoptosis. Cell Tissue Res. 2000; 301:5–17.
21. Vossenaar ER, Nijenhuis S, Helsen MM *et al.* Citrullination of synovial proteins in murine models of rheumatoid arthritis. Arthritis Rheum 2003;48:2489–500.
22. Cutolo M, Sulli A, Barone A, Seriolo B, Accardo S. Macrophages, synovial tissue and rheumatoid arthritis. Clin Exp Rheumatol 1993;11:331–9.
23. Masson-Bessiere C, Sebbag M, Girbal-Neuhauser E *et al.* The major synovial targets of the rheumatoid arthritis-specific antifilaggrin autoantibodies are deiminated forms of the alpha- and beta-chains of fibrin. J Immunol 2001;166:4177–84.
24. Weinberg JB, Pippen AM, Greenberg CS. Extravascular fibrin formation and dissolution in synovial tissue of patients with osteoarthritis and rheumatoid arthritis. Arthritis Rheum 1991;34:996–1005.
25. Sanchez-Pernaute O, Lopez-Armada MJ, Calvo E *et al.* Fibrin generated in the synovial fluid activates intimal cells from their apical surface: a sequential morphological study in antigen-induced arthritis. Rheumatology 2003;42:19–25.
26. Rantapaa-Dahlqvist S, de Jong BA, Berglin E *et al.* Antibodies against cyclic citrullinated peptide and IgA rheumatoid factor predict the development of rheumatoid arthritis. Arthritis Rheum 2003;48: 2741–9.
27. Berthelot JM, Bendaoud B, Maugars Y, Audrain M, Prost A, Youinou P. Antiperinuclear factor of the IgA isotype in active rheumatoid arthritis. Clin Exp Rheumatol 1994;12:615–9.
28. Baeten D, Peene I, Union A *et al.* Specific presence of intracellular citrullinated proteins in rheumatoid arthritis synovium: relevance to antifilaggrin autoantibodies. Arthritis Rheum 2001;44:2255–62.
29. Inagaki M, Takahara H, Nishi Y, Sugawara K, Sato C. $Ca2^{+}$-dependent deimination-induced disassembly of intermediate filaments involves specific modification of the amino-terminal head domain. J Biol Chem 1989 25;264:18119–27.
30. Schwab BL, Guerini D, Didszun C *et al.* Cleavage of plasma membrane calcium pumps by caspases: a link between apoptosis and necrosis. Cell Death Differ 2002;9:818–31.

Genes and Immunity (2005) 6, 194–202

www.nature.com/gene

FULL PAPER

CUL1, a component of E3 ubiquitin ligase, alters lymphocyte signal transduction with possible effect on rheumatoid arthritis

R Kawaida[1,3], R Yamada[1], K Kobayashi[1], S Tokuhiro[1,3], A Suzuki[1], Y Kochi[1,2], X Chang[1], A Sekine[1], T Tsunoda[1], T Sawada[2], H Furukawa[3], Y Nakamura[1] and K Yamamoto[1,2]

[1]*SNP Research Center, RIKEN, Yokohama, Kanagawa, Japan;* [2]*Graduate School of Medicine, University of Tokyo, Tokyo, Japan;* [3]*Biomedical Research Laboratories, Sankyo Co., Ltd, Tokyo, Japan*

Ubiquitination affects various immune processes and E3 ubiquitin ligases (E3) play an important role in determining substrate specificity. We identified 11 human E3 ligase genes of potential importance in pathogenesis of autoimmune diseases by search of public databases and screened them for candidacy of biological investigation with case–control linkage disequilibrium tests on multiple SNPs in the genes using rheumatoid arthritis (RA) as a model of autoimmune diseases. Significant association with RA was observed in an SNP in intron 3 of Cullin 1 (CUL1) that affected transcriptional efficiency of the promoter activity in lymphocytic cell lines. Quantitative expression analysis revealed that CUL1 mRNA was highly detected in lymphoid tissues, including spleen and tonsil, and was specifically expressed in T and B lymphocytes in fractionated peripheral leukocytes. Histological evaluation of tonsils indicated that CUL1 protein expression was relatively specific for maturing germinal centers. Suppression of CUL1 expression had influence on the phenotype of T-cell line, that is, it inhibited IL-8 induction, which is known to play an important role in the migration of inflammatory cells into the affected area seen in RA. Our data suggest that the regulation of CUL1 expression in immunological tissues may affect the susceptibility of RA via altering lymphocyte signal transduction.

Genes and Immunity (2005) **6**, 194–202. doi:10.1038/sj.gene.6364177
Published online 10 March 2005

Keywords: *rheumatoid arthritis; SNP; Cullin1; E3 ubiquitin ligase*

Introduction

The ubiquitin system contributes to many aspects of cellular activities. The length of the ubiquitin chain is generally related to different processes. Whereas at least four units of the ubiquitin chain seem necessary for proteasomal degradation,[1] mono-ubiquitination is involved in endocytosis.[2] The ubiquitin–proteasome system degrades polyubiquitinated proteins via the 26S protein complex, the proteasome. The machinery contributes to a variety of cellular processes, including cell-cycle control, signal transduction, transcriptional regulation, DNA repair, antigen presentation and apoptosis.[3] In addition to physiologically normal proteins, misfolded proteins could be substrates in the cellular stress response, through which E3s constitute a protein quality control system.[4] However, other regulatory roles such as internalization of the receptor protein,[5–7] transcription stimulation[8,9] and protein processing[10,11] via ubiquitination have recently been suggested.

Ubiquitin is a small peptide of 76 amino acids that is highly conserved in all eukaryotes. The ubiquitin pathway proceeds through a three-step enzymatic cascade involving ubiquitin-activating enzyme (E1), ubiquitin-conjugating enzyme (E2) and ubiquitin ligase (E3). While there are only dozens of E2s, E3s are highly heterogeneous. This feature allows these enzymes to determine specific ubiquitin interactions with its target proteins[12] that control cell processes such as activation, proliferation and differentiation.

The ubiquitination system is also involved in many aspects of the immune system. For example, antigens processed by polyubiquitination are presented on the surfaces of antigen-presenting cells (APCs) that are recognized by MHC class I molecules of cytotoxic T cells. Proteasome and tripeptidyl aminopeptidase II (TPPII) might cooperate to produce peptides bound by MHC class I proteins.[13,14]

E3 ubiquitin ligases are also involved in the NF-κB signaling pathway that regulates the expression of various genes during inflammation, immunity, differentiation and apoptosis. The activation cascade is also modulated by the multiple ubiquitination system

Correspondence: Dr R Yamada, Laboratory for Rheumatic Diseases, SNP Research Center, Institute of Physical and Chemical Research, 1-7-22 Suehiro-cho, Tsurumi-ku, Yokohama, Kanagawa 230-0045, Japan.
E-mail: ryamada@src.riken.go.jp
Received 15 November 2004; revised 3 January 2005; accepted 4 January 2005; published online 10 March 2005

executed by E3s. In response to proinflammatory cytokines, TRAF6 modified by polyubiquitin chains is essential for TAK1 kinase activation, which leads to IκB kinase (IKK) phosphorylation.[15,16] The activation of IKK causes the phosphorylation and degradation of IκBα, followed by NF-κB activation. The SCF (Skp1–Cullin1–Fbox)$^{\beta\text{-TrCP}}$ E3 complex participates in IκBα degradation.[17,18] Furthermore, another ubiquitin ligase might execute the proteolysis of NF-κB p105 into active subunits to translocate into the nucleus and regulate target gene transcription.[19] Recently it has been found that adaptor protein Bcl10, which is essential for NF-κB activation by T- and B-cell receptors, promotes NF-κB activation through the paracaspase- and UBC13-dependent ubiquitination of NEMO (IKK-γ).[20]

Some E3s play regulatory roles in T-cell anergy. For example, GRAIL suppresses and limits activation-induced IL-2 and IL-4 production in T-cell hybridomas.[21] The constitutive expression of GRAIL renders naive CD4T cells anergic.[22] T cells derived from E3 Itch$^{-/-}$ mice are activated and their proliferation is enhanced, which results in severe immune and inflammatory disorders and constant itching of the skin.[23] Furthermore, c-Cbl and Cbl-b negatively regulate T-cell activation by promoting the clearance of engaged TCR from the cell surface by ubiquitination,[24] and Cbl-b negatively regulates BCR signaling by targeting Syk for ubiquitination.[25]

As shown above, E3s are involved in immune processes. We identified CUL1 among E3s as a candidate of autoimmunity-related gene by screening association between SNPs and rheumatoid arthritis (RA). RA is a widespread autoimmune disease that affects 0.5–1.0% of the worldwide population. It is characterized by chronic inflammation of the synovial joints due to the infiltration of lymphocytes, macrophages and plasma cells, accompanied by hyperplasia of the synovial fibroblasts. The pathology of RA is generally defined by the activities of many inflammatory cytokines. The ubiquitin system might be involved in RA because the overexpression of the E3 ubiquitin ligase, Synoviolin/Hrd1, causes the excessive growth of synoviocytes in mice, which leads to spontaneous arthropathy.[26] One risk factor for RA is genetic contribution. The susceptibility of siblings of affected individuals and of monozygotic twins is higher than that of the general population. Genetic studies of RA using SNPs have revealed RA-susceptible SNPs such as PADI4,[27] RUNX1 and SLC22A4,[28] and PTPN22.[29] Therefore, to identify the E3s involved in autoimmune diseases, we performed a case–control linkage disequilibrium study of the Japanese RA population. We discovered an SNP associated with RA in *CUL1*, a component of the SCF E3 complex.

CUL1 is highly conserved from nematodes to humans,[30] and it is indispensable for mouse embryogenesis.[31] CUL1 binds to the Skp1–F-box protein complex and to ROC1 through its N- and C-terminal region, respectively. F-box is a member of a large family of substrate-targeting proteins that determine the specificity of E3 activity. ROC1, on the other hand, recruits an E2 enzyme and functions as a ubiquitin ligase on its substrate.[32] A structural characteristic of the E3 ligase is the RING finger motif in ROC1.[33] Besides IκBα,[17,18] SCF complex has several targets, including β-catenin,[16] p27, CyclinE1[34] and IFNα receptor 1.[6] Thus, SCF has been studied as an inflammation or/and cell cycle modulator. Here, we analyze the expression and function of CUL1 in the context of the immune system in autoimmunity.

Results

Analysis of RA-related SNPs in E3 ubiquitin ligase

Screening of E3 ubiquitin ligase genes for association with RA with SNPs. A total of 11 E3 ubiquitin ligase genes were selected as described in Materials and methods. Table 1 lists the SNPs and the genotyping results. All the SNPs were polymorphic in Japanese population, with a minor allele frequency more than 0.08% except for #31 in GRAIL. Among 33 SNPs in the 11 selected genes, only one SNP (#8) in intron 3 of the *CUL1* gene was significantly associated with RA, with $P<0.0005$ (corrected $P<0.05$ by Bonfferoni correction). Based on these results, we selected CUL1 for further analysis for function and mechanism in immune system.

SNP mapping in CUL1 locus. To investigate the region around *CUL1*, we analyzed the LD and haplotype structure with the genotype data of 40 SNPs for 94 case samples (Figure 1). SNPs with a moderately strong LD ($\Delta>0.5$) to #8 were distributed in both *CUL1* and its neighboring gene *EZH2*. We then searched for SNPs in this region using the JSNP database, which mainly focuses on SNPs in the 5′UTR, 3′UTR and the coding region.[35] We also directly sequenced 2 kb of the 5′-flanking region and exon 1, in 48 genomic samples from RA patients to find functional SNPs in the promoter region. Thus, among 40 genotyped SNPs, only intron 3 of *CUL1* contained SNPs with a *P*-value of <0.001. Furthermore, no SNPs were associated with RA in the *CUL1* coding, or 5′ and 3′ flanking regions (Figure 1). Therefore, SNP #8 in intron 3 of *CUL1* could affect susceptibility to RA. We therefore examined the functional differences of associated SNP #8.

Reporter assay of RA-associated SNP in CUL1. Reporter constructs containing one, five or nine concatenated copies of the 24 nucleotides around the associated SNP #8 were connected to the SV40 promoter (Figure 2a). The constructs were transiently transfected into both the Jurkat T-cell (Figure 2b) and Raji B-cell (Figure 2c) lines. The susceptible C allele had more enhancer activity than the nonsusceptible A allele in both cell lines, with statistical significance $P<0.005$ for five and nine concatenated constructs.

Expression of CUL1

Quantitative RT-PCR. To elucidate the role of CUL1 in inflammatory disease, we analyzed the mRNA expression level using quantitative real-time PCR. The expression levels of *CUL1* mRNA in a human tissue panel were high in the spleen, tonsils and in whole blood, and moderate in the brain, thymus, bone marrow and liver. The kidneys and heart expressed low levels of *CUL1* mRNA (Figure 3a). Synovial fibroblast cells from RA patients also expressed moderate levels of *CUL1*. Mononuclear cells in the peripheral blood expressed more *CUL1* mRNA than polynuclear cells and lymphocyte-dominant expression of CUL1 was further ascertained with expression evaluation of fractionated cells stratified with cell surface markers CD4, 8, 14 and 19 (Figure 3b).

Table 1 Summary of association of selected SNPs in E3 ubiquitin ligase between cases and controls

JSNP ID[a]	dbSNP ID[b]	Chromosome	Public location[c]	SNP_ID	Gene_name	Refseq	Structure	Case				Control				Allele 1 vs allele 2 P	Genotype 11 vs 12+22 P	Genotype 22 vs 11+12 P
								11	12	22	Sum	11	12	22	Sum			
IMS-JST084689	rs3738885	2		#1	BARD1	NM_000465.1	exon	0	57	746	803	2	39	616	657	0.6825	0.1177	0.5146
IMS-JST123390	rs3768710	2		#2	BARD1	NM_000465.1	intron	311	355	140	806	225	325	108	658	0.3457	0.0828	0.6275
IMS-JST123387	rs3768707	2		#3	BARD1	NM_000465.1	intron	56	274	471	801	41	237	367	645	0.6931	0.6315	0.4664
IMS-JST129605	rs3774206	3		#4	VHL	NM_000551.2	3′UTR	524	269	32	825	411	209	29	649	0.7949	0.9410	0.5726
—	rs1678607	3		#5	VHL	NM_000551.2	intron	522	271	32	825	408	213	28	649	0.7785	0.8724	0.6744
—	—	3	10172799	#6	IRAK2|VHL	NM_000551.2	intergene	0	3	822	825	0	3	645	648	0.7666	1.0000	0.7664
IMS-JST166832	rs243505	7		#7	CUL1	NM_003592.2	intron	401	354	69	824	299	267	84	650	0.0362	0.3090	0.0045
IMS-JST159456	rs243480	7		#8	CUL1	NM_003592.2	intron	89	378	355	822	109	298	237	644	0.0005	0.0007	0.0134
IMS-JST166838	rs3807447	7		#9	CUL1	NM_003592.2	intron	9	127	684	820	6	96	536	638	0.7194	0.7680	0.7593
IMS-JST008077	rs2072173	7		#10	SMURF1	NM_020429.1	intron	375	331	82	788	309	239	69	617	0.6258	0.3536	0.6407
IMS-JST008078	rs219797	7		#11	SMURF1	NM_020429.1	exon	350	323	108	781	249	259	89	597	0.2550	0.2491	0.5705
IMS-JST159788	rs3801241	7		#12	SMURF1	NM_020429.1	intron	63	314	430	807	47	251	358	656	0.5576	0.6432	0.6227
		8	87325448	#13	WWP1	NM_007013.3	intron	3	100	720	823	2	72	573	647	0.5268	0.8563	0.5285
—	—	8	87319229	#14	WWP1	NM_007013.3	intron	380	359	86	825	270	289	90	649	0.0245	0.0870	0.0430
—	—	8	87331177	#15	WWP1	NM_007013.3	intron	285	397	143	825	194	311	144	649	0.0097	0.0583	0.0195
IMS-JST027139	rs2279434	10		#16	c-MIR	NM_145021.2	intron	15	161	633	809	19	142	493	654	0.1137	0.1846	0.1961
IMS-JST064533	rs2306814	10		#17	c-MIR	NM_145021.2	intron	0	47	760	807	0	49	605	654	0.2085	1.0000	0.2006
IMS-JST118972	rs3764990	10		#18	c-MIR	NM_145021.2	exon	12	162	623	797	12	145	491	648	0.2640	0.6086	0.2810
IMS-JST032946	rs2283428	15		#19	UBE3A	NM_000462.2	intron	0	6	778	784	0	2	530	532	0.3732	1.0000	0.3725
—	—	15	23147683	#20	UBE3A	NM_000462.2	intron	333	373	119	825	261	300	87	648	0.7989	0.9734	0.5834
—	—	15	23218664	#21	UBE3A	NM_000462.2	intron	120	374	330	824	88	300	261	649	0.7438	0.5829	0.9482
IMS-JST100147	rs3748401	16		#22	AMFR	NM_001144.3	exon	6	105	682	793	4	85	568	657	0.7568	0.7350	0.8042
IMS-JST100149	rs2617846	16		#23	AMFR	NM_001144.3	intron	221	383	202	806	181	330	146	657	0.4239	0.9558	0.2045
IMS-JST100150	rs2617847	16		#24	AMFR	NM_001144.3	intron	108	348	254	710	56	188	132	376	0.9367	0.8894	0.8267
IMS-JST039538	rs2288339	17		#25	SMURF2	NM_022739.2	intron	23	220	545	788	19	129	348	496	0.9771	0.3711	0.7049
IMS-JST060286	rs2303572	17		#26	SMURF2	NM_022739.2	intron	712	40	0	752	476	28	1	505	0.6425	0.7466	0.2222
IMS-JST060287	rs2303573	17		#27	SMURF2	NM_022739.2	intron	692	43	0	735	463	29	0	492	0.9748	0.9744	1.0000
IMS-JST114708	rs3761147	20		#28	ITCH	NM_031483.3	intron	367	342	97	806	284	306	60	650	0.7837	0.4824	0.0864
—	rs2424992	20		#29	ITCH	NM_031483.3	intron	373	352	99	824	290	283	75	648	0.9833	0.8440	0.7950
—	rs3746455	20		#30	ITCH	NM_031483.3	UTR 5	373	351	99	823	292	281	75	648	0.9556	0.9207	0.7885
—	rs5962358	X		#31	GRAIL	NM_194463.1	intron	823	0	0	823	645	0	0	645	N. D.	1.0000	1.0000
—	rs6523888	X		#32	GRAIL	NM_194463.1	intron	0	3	821	824	0	1	646	647	0.4440	1.0000	0.4437
—	rs2880013	X		#33	GRAIL	NM_194463.1	intron	456	266	103	825	410	134	105	649	0.2050	0.0022	0.0432

[a]JSNP database.
[b]National Center for Biotechnology Information (NCBI) dbSNP database.
[c]Location of SNP based on chromosomal data in Build34.

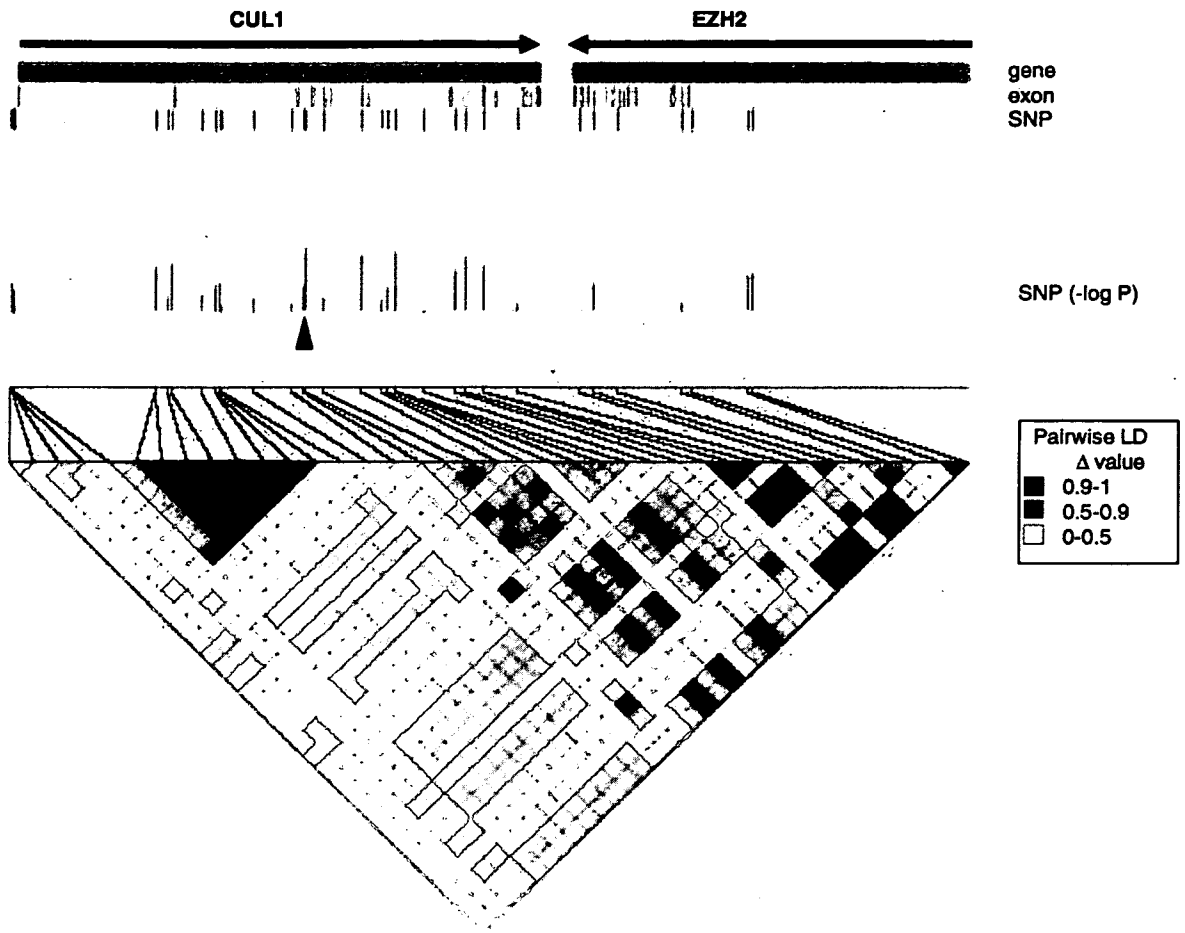

Figure 1 LD map and genomic structure of *CUL1*. Location of genes, exons, SNPs and $-\log P$ values of SNP in *CUL1* and *EZH2* regions. Arrow indicates the direction of gene. Arrowhead indicates the location of #8, which has the strongest association in this region. Pairwise LD between SNPs in NT_007914.13, as measured by Δ in 94 case samples was shown.

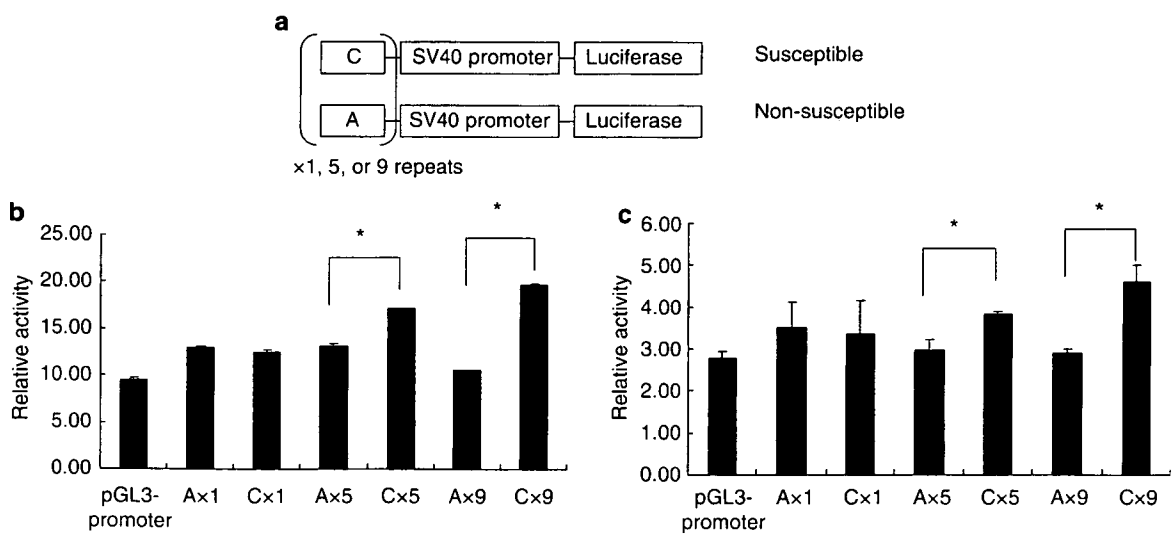

Figure 2 Comparison of allelic variants of #8 in *CUL1* by reporter luciferase assay. (**a**) Reporter plasmid constructs. Relative luciferase activities of transiently transfected constructs in Jurkat (**b**) and Raji (**c**) cells. Data show means ± s.d. of triplicates. $^*P < 0.005$ by Student's *t*-test.

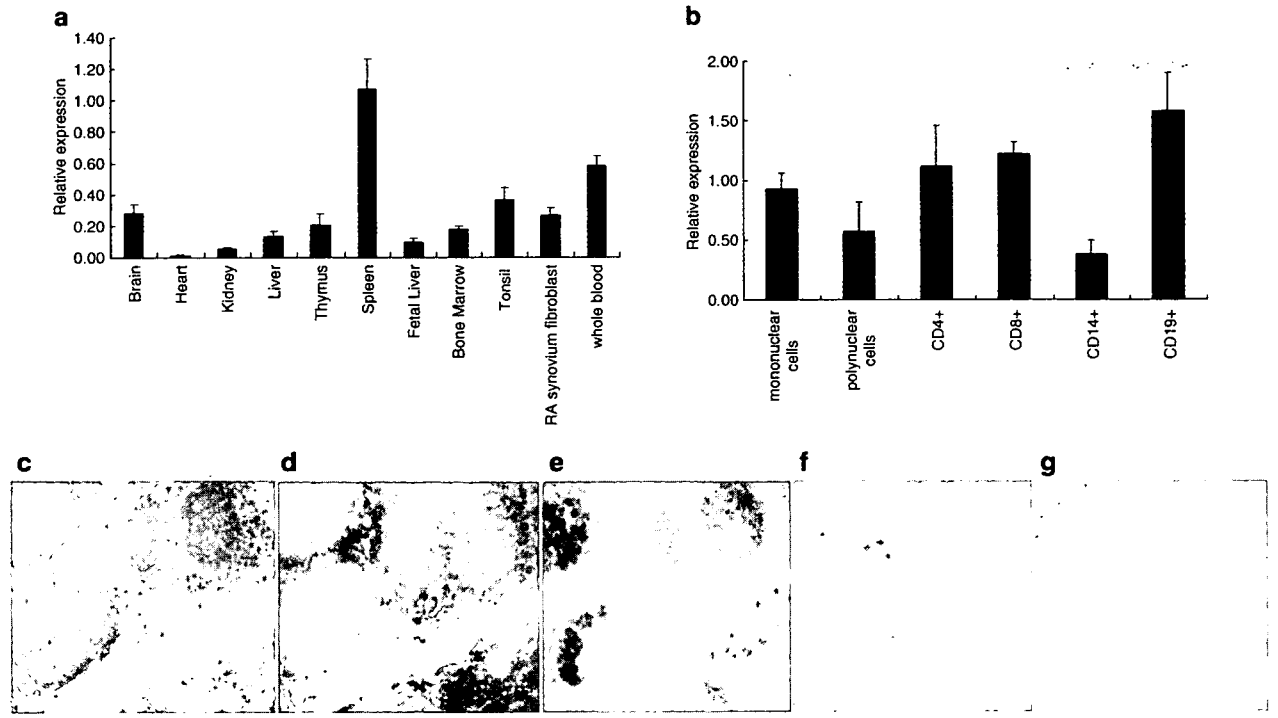

Figure 3 Expression of CUL1. Relative expression levels of *CUL1* in various human tissues (**a**) and in fractionated blood cells (**b**) analyzed by quantitative real-time PCR. Data show means±s.d. relative expression in triplicate. (**c–g**) Distribution of CUL1 protein in tonsil. Serial sections of human tonsils immunohistochemically stained as described in Materials and methods with anti-CD20 (**c**), anti-CD3 (**d**), anti-CD23 (**e**), anti-CUL1 (**f**) and isotype control rabbit IgG (**g**).

Immunohistochemistry. To further investigate subtypes of lymphocytes expressing CUL1, we examined tonsil sections using immunohistochemical staining (Figure 3c–g). Well-structured germinal centers were observed in the sections with hematoxylin-eosin staining (data not shown) and anti-CD20 and anti-CD3 antibody staining (Figure 3c and d respectively). Germinal centers were immunohistologically divided into two types. One type was clearly structured with CD23-positive cells, and the other was not. We counted 30 CD23-positive germinal centers and 14 CD23-negative germinal centers (Figure 3e). Although expression of CUL1 was principally detected in germinal centers, where B-cells dominated (Figure 3f), not all germinal centers were positive with anti-CUL1 antibody signal. CUL1-positive fraction among germinal centers was 77% (34 out of 44) and the ratio was different between CD23-positive and -negative germinal centers. CUL1-positive germinal centers were more likely to be CD23-positive (28 out of 30) than CD23-negatives (six out of 14). The difference seemed to indicate that CUL1 expression was regulated along with germinal center maturation.

CUL1 siRNA inhibits IL-8 production in Jurkat cells

To investigate the role of CUL1 in lymphocytic cells, we interrupted *CUL1* expression by siRNA transfection. Transfection of siRNA into Jurkat cells induced decrease of CUL1 protein with dose dependency and the decrease was observed 24 h after transfection, and it persisted up to 72 h after the transfection. Suppression of ubiquitination activity of the SCF complex was measured by accumulation of p27, which was a known substrate of the Roc1–Skp1–CUL1–F-box (Skp2) complex (Figure 4a). As a control to evaluate substrate specificity, we used the CDK2 protein that interacts with p27 in the G1 to S transition state and is not degraded by the complex.[36] In contrast to p27, CDK2 kept a steady level in spite of *CUL1* siRNA transfection. The specificity of the siRNA was confirmed by lack of change in the amount of CUL1 and p27 protein by transfection of a control siRNA against the luciferase gene. IL-8 is one of the cytokines that are known to be induced in T cells by various stimulations. As shown in Figure 4b, *CUL1* siRNA significantly suppressed *IL-8* mRNA induction in Jurkat cells stimulated with PMA and PHA in a dose-dependent manner (Figure 4b) ($P<0.05$).

Discussion

The present study showed that the regulation of E3 ubiquitin ligase CUL1 expression in immunological tissues might affect susceptibility to autoimmune RA via an associated SNP in intron 3 of *CUL1*. We searched the databases for SNP in the *CUL1* gene and its regulatory region from the promoter and from the first to the last exon including the intron.[35] However, we found SNPs only in the intron region. As *CUL1* is highly conserved among organisms and plays an important role in mice embryogenesis,[31] the molecular functions of CUL1 as a component of the E3 ligase complex should be strictly regulated both qualitatively and quantitatively *in vivo*. We evaluated a sequence from 2 kb upstream from the transcription initiation site and exon 1 for the

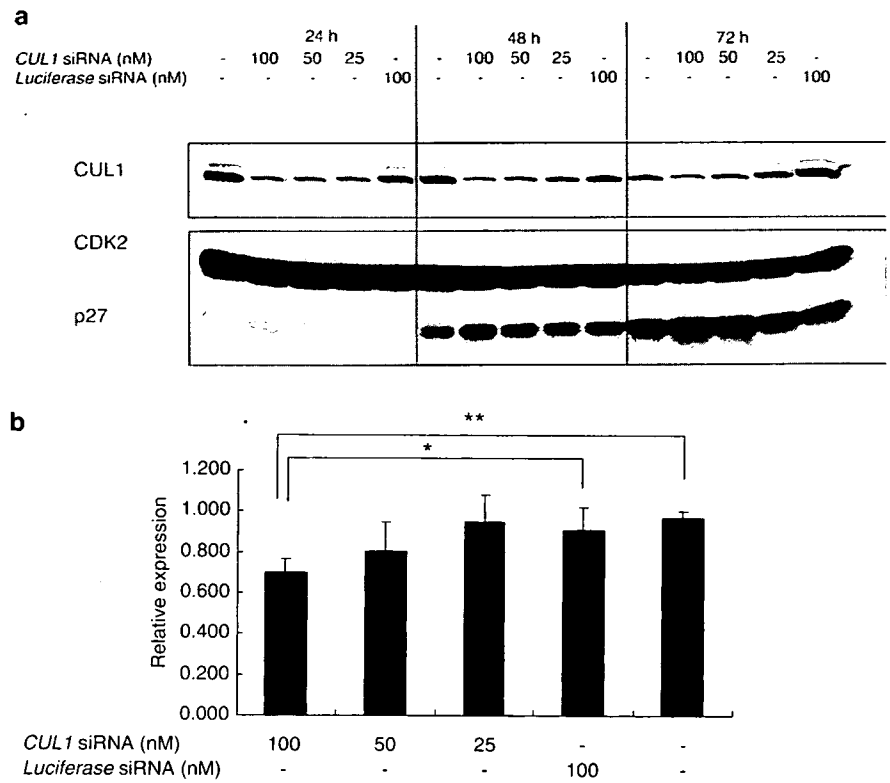

Figure 4 Suppression of *IL-8* induction by siRNA to *CUL1* in Jurkat cells. Confirmation of siRNA effect against *CUL1*. Time course of Western blots using antibody against CUL1, CDK2 and p27. Relative expression level of *IL-8* mRNA in Jurkat cells stimulated PMA and PHA as described in Materials and methods. Data show means ± s.d. of triplicates. $^{*}P<0.05$ and $^{**}P<0.005$ by Student's *t*-test.

presence of SNPs in the region with regulatory elements. However, a functional SNP which had association with RA was never found in the coding or promoter regions of *CUL1* (Figure 1). The associated SNP in intron 3 is probably involved in the subtle control of expression and might affect common disease susceptibility.

Expression profiling revealed high levels of *CUL1* expression in the spleen and tonsils, as well as in the T- and B-cell fraction of whole blood (Figure 3a and b). Therefore, CUL1 might function as a modulator in the development and activation status of hematological cells. In addition, since CUL1 is involved in the regulation of centrosome replication in *Drosophila* neuroblasts,[37] moderate expression in the brain and liver might contribute to appropriate cell division in these tissues. From the viewpoint of lymphoid tissue, introducing the dominant-negative form of CUL1 into T-lineage cells causes lymphoid organ hypoplasia and reduced proliferation, followed by abnormal cell division.[36] Therefore, CUL1 contributes to T-lymphocyte division and proliferation. The relatively low level of *CUL1* expression in CD14-positive monocytic cells suggests that another factor(s) plays a role in cell proliferation and/or NF-κB activation in addition to CUL1. We showed how CUL1 protein is expressed in human tonsils. In such secondary lymphoid tissues, germinal centers are specialized for the selection of antigen-specific B cells that leads to extensive expansion, isotype switching, somatic hypermutation and differentiation into plasma cells and memory cells. Germinal centers arise when B cells accumulate among the processes of follicular dendritic cells and undergo intense proliferation, apoptosis and hypermutation. B cells that produce high-affinity antibodies in response to antigen presented by T cells are selected to survive, while B cells that do not recognize antigen enter apoptosis.[38] In this structure, CD23 is an early-activation antigen marker of normal and activated B cells of the mantle zone, and follicular dendritic reticulum cells can be visualized by intense staining. The expression of CUL1 protein overlapped with CD20-positive B cells rather than CD3-positive T cells in the CD23-positive germinal center structure (Figure 3c–f). Germinal center structures are ectopically generated in RA synovium tissue.[39] Therefore, CUL1 must play a role in B cells of mature, differentiated germinal centers during autoimmune status. This might help not only immature B cells to rapidly divide and cause B-cell expansion, but also mature B cells to survive through NF-κB activation.

The intron region in addition to SNPs in the promoter region might be involved in regulating the expression level of the gene. For example, SNPs in intron 1 of LGALS2[40] and LT-α[41] cause changes in transcriptional activity. A relationship between a sequence in the intron region and a ligand-responsive element has also been indicated in the ATP-binding cassette transporter G1.[42] We searched the promoter and exon region of *CUL1*, but did not detect any SNPs. As *CUL1* is highly conserved, subtle changes in the intron region should affect expression levels of the gene. Therefore, we investigated the influence of SNP in intron 3 of *CUL1* on transcriptional

efficiency in lymphocytic cell lines. Allelic differences in SNP #8 in intron 3 influenced the enhancer-like activity in both T- and B-cell lines (Figure 2). These results from reporter assays and expression profiling indicate that #8 can affect the expression level of *CUL1* in immunological tissues. Changing one nucleotide within the site from A (nonsusceptible allele) to C (susceptible allele) in #8 generated a score indicating that the binding probability to Ets-1 in the TRANSFAC databases[43] would increase from 71.1 to 87.0, respectively. Ets-1 might regulate T-cell survival and activation, as well as B-cell differentiation status.[44,45] Enhanced *CUL1* expression due to Ets-1 binding in intron 3 might alter T- and B-cell behavior in immunological tissue and/or blood that would cause a change to autoimmune status as described above.

To investigate the role of CUL1 in lymphoid cells, we suppressed *CUL1* mRNA transcription by transfecting siRNA into a Jurkat T-cell line. This partially decreased the induction of IL-8 mRNA by PMA and PHA (Figure 4). IL-8 is a cytokine with both chemotactic and angiogenic effects produced by T lymphocytes following activation. Transcription factor-binding sites have been identified in the promoter of the *IL-8* gene. The sequence contains binding sequences for AP-1, C/EBP and NF-κB and confers an IL-8 promoter response to IL-1, TNF and PMA.[46] In addition, enhanced IL-8 production in RA synovial fibroblasts stimulated with IL-17 is transduced both via NF-κB and PI3-kinase/Akt.[47] The expression of IL-8 was partially inhibited probably due to accumulation of the CUL1 substrate IκBα, which leads to NF-κB inactivation. However, IL-2 and TNFα were not inhibited by siRNA (data not shown). The regulation of these cytokine levels might depend more on factors other than NF-κB when stimulated with PMA and PHA. These data suggest that CUL1 positively regulates chemokine IL-8 production by T cells in immunological tissues. Although B-cell lines were not functionally analyzed due to transfection difficulties, B-cell signaling might also be affected and altered by changes in CUL1 expression levels in structures like germinal centers during autoimmune status. B cells expressing higher levels of CUL1 probably tend to escape apoptosis through NF-κB hyperactivation.

In conclusion, we found that *CUL1* is an E3 ubiquitin ligase that is predominantly expressed in T and B lymphocytes and its expression seems to be regulated by functional differentiation of lymphocytes. It might be responsible for susceptibility to RA through altering lymphocyte signal transduction. Comparisons of CUL1 expression between individuals with susceptible and nonsusceptible alleles and the generation of tissue-specific CUL1 knockdown and/or transgenic mice should help to define the role of CUL1 in autoimmune diseases.

Materials and methods

SNPs and genotyping E3 ubiquitin ligase genes

We screened E3 ubiquitin ligases as follows. Firstly, we searched NCBI Entrez Nucleotide database with keywords 'E3 ubiquitin ligase', 'Homo sapiens' (organism), 'biomol_mrna' (PROP) and 'srcdb_refseq' (PROP) and identified 91 human transcript nucleotide sequences. Among the 91 hits, we selected only 24 genes whose encoding proteins were previously reported to have E3 ubiquitin ligase activity by manually inspecting reference reports. We then scrutinized the genes using the SAGE Anatomic Viewer in the NCI Gene Finder Database. We finally selected 11 genes that express more than four clones per 200 000 clones from either lymph node or white blood cells. We selected 88 SNPs in these genes both by JSNP[35] and NCBI dbSNP databases. We recruited Japanese individuals with and without RA as described.[27] Using 94 case samples, we genotyped 88 SNPs and analyzed linkage disequilibrium (LD). Based on the results, we finally selected three SNPs per gene, which were mutually as independent as possible from the LD standpoint. We genotyped the selected 33 SNPs in 11 genes for 846 cases and 658 controls by Invader[48] or TaqMan[27] assays with probe sets designed and synthesized by Third Wave Technologies and by Applied Biosystems, respectively. Association was tested with χ^2 test or Fisher's exact test.

Cell culture

Jurkat E6-1 and Raji cells in RPMI1640 (Life Technologies) supplemented with 10% heat-inactivated (56°C for 30 min) FCS (JRH Biosciences) were maintained at 37°C in a humidified 5% CO_2 atmosphere. Both cell lines were purchased from ATCC.

Reagents

We purchased Human Blood Fractions from the MTC Panel, human total RNA from Clontech, and PMA and PHA from Sigma.

Antibodies

A polyclonal antibody against human CUL1 and horseradish peroxidase-linked anti-rabbit IgG were purchased from Lab Vision and Amersham Pharmacia Biotech, respectively. Anti-CD23 mAb was obtained from MBL. Anti-CD3 and anti-CD20 mAbs were obtained from Zymed. Isotype control rabbit IgG and anti-CDK2 mAb were purchased from Santa Cruz and anti-p27 mAb was from BD Biosciences.

Immunohistochemistry

Human tonsil sections (Genomics Collaborative Global Repository) were deparaffinized and then rehydrated in xylene and a graded ethanol series. After heating in Target Retrieval Solution (Dako Cytomation) for 40 min at 95°C, endogenous peroxidase was quenched in 0.3% peroxide in PBS for 1 h and then nonspecific binding was blocked with Fc Receptor Blocker (Innovex). The sections were then stained using the Universal Elite ABC kit and a DAB substrate kit (Vector Laboratories) according to the manufacturer's instructions. Nuclei were counterstained with hematoxylin.

Western blotting

To prepare whole cell extracts, cells were washed with phosphate-buffered saline, lysed in RIPA buffer (1% NP-40, 0.5% deoxycholic acid and 0.1% SDS in phosphate-buffered saline) supplemented with complete protease inhibitor cocktail (Roche Diagnostics), and then sedimented by centrifugation. Equal amounts of protein (10–15 μg) from the supernatant were separated in 5–20% gradient SDS-polyacrylamide gels and then electroblotted onto a polyvinylidene difluoride membrane

(Bio-Rad). Proteins of interest were visualized using the ECL Plus Western blotting detection system (Amersham Pharmacia Biotech) according to the manufacturer's instructions.

Luciferase assay

Luciferase reporter plasmids were constructed by cloning single, five or nine concatenated copies of the adjacent 24 nucleotides of the SNP #8 nucleotide into the pGL3-promoter vector (Promega) upstream of the SV40 promoter. We also introduced *Kpn*I or *Nhe*I sites at the 5′ ends of sense or antisense oligonucleotides, respectively. The fidelity of the constructs was verified by nucleotide sequencing. Jurkat cells were transfected with 2 μg of either of the constructs and with 0.2 μg of the pRL-TK *Renilla* luciferase vector (Promega) to normalize transfection efficiency using DMRIE-C reagent (Invitrogen). After 5 h, the cells were incubated with PHA and PMA at final concentrations of 1 μg/ml and 50 ng/ml, respectively, for 16 h. Raji cells were transfected with the same plasmids described above using the A-23 program of Amaxa Nucleofector™ (Amaxa) according to the manufacturer's instructions. The cells were incubated on the following day for 5 h with the same concentration of PHA and PMA as the Jurkat cells, and then cell extracts were prepared using Passive Lysis Buffer (Promega). Firefly and *Renilla* luciferase activities in the cell lysates were determined using a Dual-luciferase assay system (Promega) according to the supplier's instructions.

RNA interference assay

An RNA consisting of 21 nucleotides was chemically synthesized (TaKaRa) and the various amounts of siRNA was transiently transfected with C-16 program using the Amaxa Nucleofector™ (Amaxa) according to the manufacturer's instructions. Cells were incubated on the following day with PHA and PMA at final concentrations of 1 μg/ml and 50 ng/ml, respectively, for 5 h. Total RNA was then extracted using the RNeasy Mini kit and an RNase-Free DNase set (QIAGEN) according to the instruction manual provided. First-strand cDNA was synthesized using oligo $d(T)_{16}$ primers and TaqMan Reverse Transcription Reagents (Applied Biosystems).

Quantitative real-time PCR

TaqMan PCR proceeded using an ABI PRISM 7900 Sequence Detection System (Applied Biosystems) according to the manufacturer's instructions. TaqMan probes and primers were Assays-on-Demand gene expression products (Applied Biosystems). Preparation of rheumatoid synovial fibroblasts has been described.[49] The relative expression of *CUL1* and *IL-8* mRNA was normalized to the amount of *GAPDH* in the same cDNA using a standard curve or the ΔΔ method according to the manufacturer's instructions.

Acknowledgements

We thank members of the Laboratory for Rheumatic Diseases for their technical assistance; H Kawakami and T Kawaguchi for their computer programming; S Yoshino for clinical samples; K Watanabe and T Hirai for assistance in search of various kinds of databases; M Ono, T Takahashi, T Ohtsuka and M Nakayama for discussions. This work was supported by a grant from the Japanese Millenium Project.

References

1 Pickart CM. Back to the future with ubiquitin. *Cell* 2004; **116**: 181–190.
2 Hicke L, Dunn R. Regulation of membrane protein transport by ubiquitin and ubiquitin-binding proteins. *Annu Rev Cell Dev Biol* 2003; **19**: 141–172.
3 Hershko A, Ciechanover A. The ubiquitin system. *Annu Rev Biochem* 1998; **67**: 425–479.
4 Hatakeyama S, Nakayama KI. U-box proteins as a new family of ubiquitin ligases. *Biochem Biophys Res Commun* 2003; **302**: 635–645.
5 Marchese A, Raiborg C, Santini F, Keen JH, Stenmark H, Benovic JL. The E3 ubiquitin ligase AIP4 mediates ubiquitination and sorting of the G protein-coupled receptor CXCR4. *Dev Cell* 2003; **5**: 709–722.
6 Kumar KG, Tang W, Ravindranath AK, Clark WA, Croze E, Fuchs SY. SCF(HOS) ubiquitin ligase mediates the ligand-induced down-regulation of the interferon-alpha receptor. *EMBO J* 2003; **22**: 5480–5490.
7 Soubeyran P, Kowanetz K, Szymkiewicz I, Langdon WY, Dikic I. Cbl–CIN85–endophilin complex mediates ligand-induced downregulation of EGF receptors. *Nature* 2002; **416**: 183–187.
8 Miyazaki K, Ozaki T, Kato C *et al*. A novel HECT-type E3 ubiquitin ligase, NEDL2, stabilizes p73 and enhances its transcriptional activity. *Biochem Biophys Res Commun* 2003; **308**: 106–113.
9 Takano Y, Adachi S, Okuno M *et al*. The RING finger protein, RNF8, interacts with retinoid X receptor {alpha} and enhances Its transcription-stimulating activity. *J Biol Chem* 2004; **279**: 18926–18934.
10 Heissmeyer V, Krappmann D, Hatada EN, Scheidereit C. Shared pathways of I{kappa}B kinase-induced SCF{beta}TrCP-mediated ubiquitination and degradation for the NF-{kappa}B precursor p105 and I{kappa}B{alpha}. *Mol Cell Biol* 2001; **21**: 1024–1035.
11 Amir RE, Iwai K, Ciechanover A. The NEDD8 pathway is essential for SCFbeta-TrCP-mediated ubiquitination and processing of the NF-kappa B precursor p105. *J Biol Chem* 2002; **277**: 23253–23259.
12 Pickart CM. Mechanisms underlying ubiquitination. *Annu Rev Biochem* 2001; **70**: 503–533.
13 Kloetzel PM, Ossendorp F. Proteasome and peptidase function in MHC-class-I-mediated antigen presentation. *Curr Opin Immunol* 2004; **16**: 76–81.
14 Kloetzel PM. Generation of major histocompatibility complex class I antigens: functional interplay between proteasomes and TPPII. *Nat Immunol* 2004; **5**: 661–669.
15 Deng L, Wang C, Spencer E *et al*. Activation of the IkappaB kinase complex by TRAF6 requires a dimeric ubiquitin-conjugating enzyme complex and a unique polyubiquitin chain. *Cell* 2000; **103**: 351–361.
16 Wang C, Deng L, Hong M, Akkaraju GR, Inoue J, Chen ZJ. TAK1 is a ubiquitin-dependent kinase of MKK and IKK. *Nature* 2001; **412**: 346–351.
17 Nakayama K, Hatakeyama S, Maruyama S *et al*. Impaired degradation of inhibitory subunit of NF-{kappa}B (I{kappa}B) and {beta}-catenin as a result of targeted disruption of the {beta}-TrCP1 gene. *Proc Natl Acad Sci USA* 2003; **100**: 8752–8757.
18 Fuchs SY, Chen A, Xiong Y, Pan ZQ, Ronai Z. HOS, a human homolog of Slimb, forms an SCF complex with Skp1 and Cullin1 and targets the phosphorylation-dependent degradation of IkappaB and beta-catenin. *Oncogene* 1999; **18**: 2039–2046.

19 Cohen S, Achbert-Weiner H, Ciechanover A. Dual effects of I{kappa}B kinase {beta}-mediated phosphorylation on p105 fate: SCF{beta}-TrCP-dependent degradation and SCF{beta}-TrCP-independent processing. *Mol Cell Biol* 2004; **24**: 475–486.
20 Wertz IE, O'Rourke KM, Zhou H *et al*. De-ubiquitination and ubiquitin ligase domains of A20 downregulate NF-{kappa}B signalling. *Nature* 2004; **430**: 694–699.
21 Anandasabapathy N, Ford GS, Bloom D *et al*. GRAIL: an E3 ubiquitin ligase that inhibits cytokine gene transcription is expressed in anergic CD4+ T cells. *Immunity* 2003; **18**: 535–547.
22 Seroogy CM, Soares L, Ranheim EA *et al*. The gene related to anergy in lymphocytes, an E3 ubiquitin ligase, is necessary for anergy induction in CD4T cells. *J Immunol* 2004; **173**: 79–85.
23 Fang D, Elly C, Gao B *et al*. Dysregulation of T lymphocyte function in itchy mice: a role for Itch in TH2 differentiation. *Nat Immunol* 2002; **3**: 281–287.
24 Naramura M, Jang IK, Kole H, Huang F, Haines D, Gu H. c-Cbl and Cbl-b regulate T cell responsiveness by promoting ligand-induced TCR down-modulation. *Nat Immunol* 2002; **3**: 1192–1199.
25 Sohn HW, Gu H, Pierce SK. Cbl-b negatively regulates B cell antigen receptor signaling in mature B cells through ubiquitination of the tyrosine kinase Syk. *J Exp Med* 2003; **197**: 1511–1524.
26 Amano T, Yamasaki S, Yagishita N *et al*. Synoviolin/Hrd1, an E3 ubiquitin ligase, as a novel pathogenic factor for anthropathy. *Genes Dev* 2003; **17**: 2436–2449.
27 Suzuki A, Yamada R, Chang X *et al*. Functional haplotypes of PADI4, encoding citrullinating enzyme peptidylarginine deiminase 4, are associated with rheumatoid arthritis. *Nat Genet* 2003; **34**: 395–402.
28 Tokuhiro S, Yamada R, Chang X *et al*. An intronic SNP in a RUNX1 binding site of SLC22A4, encoding an organic cation transporter, is associated with rheumatoid arthritis. *Nat Genet* 2003; **35**: 341–348.
29 Begovich AB, Carlton VE, Honigberg LA *et al*. A missense single-nucleotide polymorphism in a gene encoding a protein tyrosine phosphatase (PTPN22) is associated with rheumatoid arthritis. *Am J Hum Genet* 2004; **75**: 330–337.
30 Kipreos ET, Lander LE, Wing JP, He WW, Hedgecock EM. cul-1 is required for cell cycle exit in *C. elegans* and identifies a novel gene family. *Cell* 1996; **85**: 829–839.
31 Dealy MJ, Nguyen KV, Lo J *et al*. Loss of Cul1 results in early embryonic lethality and dysregulation of cyclin E. *Nat Genet* 1999; **23**: 245–248.
32 Wu K, Fuchs SY, Chen A *et al*. The SCFHOS/beta-TRCP-ROC1 E3 ubiquitin ligase utilizes two distinct domains within CUL1 for substrate targeting and ubiquitin ligation. *Mol Cell Biol* 2000; **20**: 1382–1393.
33 Pan ZQ, Kentsis A, Dias DC, Yamoah K, Wu K. Nedd8 on cullin: building an expressway to protein destruction. *Oncogene* 2004; **23**: 1985–1997.
34 Nakayama K, Nagahama H, Minamishima YA *et al*. Targeted disruption of Skp2 results in accumulation of cyclin E and p27(Kip1), polyploidy and centrosome overduplication. *EMBO J* 2000; **19**: 2069–2081.
35 Haga H, Yamada R, Ohnishi Y, Nakamura Y, Tanaka T. Gene-based SNP discovery as part of the Japanese Millennium Genome Project: identification of 190 562 genetic variations in the human genome. Single-nucleotide polymorphism. *J Hum Genet* 2002; **47**: 605–610.
36 Piva R, Liu J, Chiarle R, Podda A, Pagano M, Inghirami G. *In vivo* interference with Skp1 function leads to genetic instability and neoplastic transformation. *Mol Cell Biol* 2002; **22**: 8375–8387.
37 Wojcik EJ, Glover DM, Hays TS. The SCF ubiquitin ligase protein slimb regulates centrosome duplication in *Drosophila*. *Curr Biol* 2000; **10**: 1131–1134.
38 Guzman-Rojas L, Sims-Mourtada JC, Rangel R, Martinez-Valdez H. Life and death within germinal centres: a double-edged sword. *Immunology* 2002; **107**: 167–175.
39 Weyand CM, Goronzy JJ. Ectopic germinal center formation in rheumatoid synovitis. *Ann NY Acad Sci* 2003; **987**: 140–149.
40 Ozaki K, Inoue K, Sato H *et al*. Functional variation in LGALS2 confers risk of myocardial infarction and regulates lymphotoxin-[alpha] secretion *in vitro*. *Nature* 2004; **429**: 72–75.
41 Ozaki K, Ohnishi Y, Iida A *et al*. Functional SNPs in the lymphotoxin-alpha gene that are associated with susceptibility to myocardial infarction. *Nat Genet* 2002; **32**: 650–654.
42 Nakamura K, Kennedy MA, Baldan A, Bojanic DD, Lyons K, Edwards PA. Expression and regulation of multiple murine ATP-binding cassette transporter G1 mRNAs/isoforms that stimulate cellular cholesterol efflux to high density lipoprotein. *J Biol Chem* 2004; **279**: 45980–45989.
43 Heinemeyer T, Wingender E, Reuter I *et al*. Databases on transcriptional regulation: TRANSFAC, TRRD and COMPEL. *Nucleic Acids Res* 1998; **26**: 362–367.
44 Bories JC, Willerford DM, Grevin D *et al*. Increased T-cell apoptosis and terminal B-cell differentiation induced by inactivation of the Ets-1 proto-oncogene. *Nature* 1995; **377**: 635–638.
45 Muthusamy N, Barton K, Leiden JM. Defective activation and survival of T cells lacking the Ets-1 transcription factor. *Nature* 1995; **377**: 639–642.
46 Mukaida N, Mahe Y, Matsushima K. Cooperative interaction of nuclear factor-kappa B- and *cis*-regulatory enhancer binding protein-like factor binding elements in activating the interleukin-8 gene by pro-inflammatory cytokines. *J Biol Chem* 1990; **265**: 21128–21133.
47 Hwang SY, Kim JY, Kim KW *et al*. IL-17 induces production of IL-6 and IL-8 in rheumatoid arthritis synovial fibroblasts via NF-kappaB- and PI3-kinase/Akt-dependent pathways. *Arthritis Res Ther* 2004; **6**: R120–R128.
48 Ohnishi Y, Tanaka T, Ozaki K, Yamada R, Suzuki H, Nakamura Y. A high-throughput SNP typing system for genome-wide association studies. *J Hum Genet* 2001; **46**: 471–477.
49 Miyazawa K, Mori A, Yamamoto K, Okudaira H. Transcriptional roles of CCAAT/enhancer binding protein-beta, nuclear factor-kappaB, and C-promoter binding factor 1 in interleukin (IL)-1beta-induced IL-6 synthesis by human rheumatoid fibroblast-like synoviocytes. *J Biol Chem* 1998; **273**: 7620–7627.

ARTHRITIS & RHEUMATISM
Vol. 52, No. 6, June 2005, pp 1920–1928
DOI 10.1002/art.21040

Angiotensin Receptor Blockers Suppress Antigen-Specific T Cell Responses and Ameliorate Collagen-Induced Arthritis in Mice

Kayo Sagawa, Katsuya Nagatani, Yoshinori Komagata, and Kazuhiko Yamamoto

Objective. **The renin–angiotensin system plays an important role in the regulation of cardiovascular, renal, and endocrine functions. Recent studies have demonstrated that angiotensin II has proinflammatory effects that may contribute to the pathogenesis of immune-mediated diseases. We used the collagen-induced arthritis (CIA) model to investigate the influence of angiotensin II receptor blockers (ARBs) on antigen-specific immune responses and determine whether ARBs have preventive or therapeutic effects on the development of arthritis.**

Methods. **We administered ARBs (olmesartan, candesartan, and telmisartan) to mice and evaluated antigen-specific T cell proliferation and cytokine production following immunization with ovalbumin (OVA) or type II collagen in Freund's complete adjuvant (CFA) or aluminum hydroxide (alum). Next, we induced CIA in DBA/1 mice and administered olmesartan. The severity and incidence of arthritis were scored according to clinical manifestations, and joint tissue sections were examined histopathologically.**

Results. **ARBs severely suppressed lymphocyte proliferation and interferon-γ production in mice immunized with OVA or type II collagen in CFA. Olmesartan also suppressed lymphocyte proliferation in mice immunized with ovalbumin in alum. In the CIA model, olmesartan reduced the mean arthritis score and the incidence of severe arthritis, even when it was administered only after disease onset. Histopathologic findings for joint destruction were improved in olmesartan-treated mice.**

Conclusion. **ARBs suppressed antigen-specific immune responses for Th1 and Th2 in vivo. Furthermore, olmesartan suppressed the development of severe arthritis and joint destruction in the CIA model. These findings suggest that ARBs may have therapeutic potential in rheumatoid arthritis.**

The renin–angiotensin system (RAS) plays an important role in the regulation of blood pressure and fluid homeostasis. Two distinct subclasses of the angiotensin II (Ang II) receptors, AT_1 and AT_2, have been described (1,2). Ang II, the major biologically active peptide produced by the RAS, causes cell proliferation and fibrosis via the AT_1 receptor and is a factor in various diseases such as hypertension, glomerular disease, and congestive heart failure (3,4).

Emerging evidence suggests that the RAS, in addition to promoting cell growth and proliferation, may also have potent proinflammatory effects that contribute to disease pathogenesis. For example, Shao et al (5) showed that levels of the Th1 cytokine interferon-γ (IFNγ) increased and those of the Th2 cytokine interleukin-4 (IL-4) decreased in Ang II–infused hypertensive rats with kidney injury, and that the administration of olmesartan, an Ang II receptor blocker (ARB), corrected this imbalance of Th subsets. Ruiz-Ortega et al (6–8) showed that Ang II activated NF-κB and up-regulated NF-κB–related genes both in vivo and in vitro.

Moreover, several recent studies demonstrated the protective effect of RAS antagonists in immunologically mediated diseases. For example, some groups of investigators demonstrated that ARBs significantly ameliorated kidney injury in rat models of chronic renal allograft rejection (9–11). In a model of chronic rejection of cardiac allografts, ARBs significantly amelio-

Kayo Sagawa, MD, Katsuya Nagatani, MD, PhD, Yoshinori Komagata, MD, Kazuhiko Yamamoto, MD, PhD: University of Tokyo, Tokyo, Japan.

Drs. Sagawa and Nagatani contributed equally to this work.

Address correspondence and reprint requests to Yoshinori Komagata, MD, Department of Allergy and Rheumatology, Graduate School of Medicine, University of Tokyo, 7-3-1 Hongo, Bunkyo-ku, Tokyo 113-8655, Japan. E-mail: komagata-tky@umin.ac.jp.

Submitted for publication June 12, 2004; accepted in revised form February 18, 2005.

rated intimal proliferation of coronary arteries, which is a pathologic finding in the setting of chronic rejection (12). Furthermore, it was reported that captopril, an angiotensin-converting enzyme (ACE) inhibitor, improved arthritis symptoms, clinical scores, plasma viscosity, and the C-reactive protein level in patients with active rheumatoid arthritis (RA) (13). In addition, Godsel et al (14) recently reported that captopril ameliorated experimental autoimmune myocarditis. These studies identified potent effects of the RAS in modulating the immune system.

Nataraj et al (15) reported that the actions of Ang II in stimulating lymphocyte proliferation played a role in modulating immune responses, and that the stimulation of AT_1 receptors on lymphocytes led to an increase in the intracellular calcium concentration. Furthermore, those investigators observed that this AT_1-mediated calcium signal triggered the activation of calcineurin and nuclear factor of activated T cells, and that cyclosporine, a specific inhibitor of calcineurin phosphatase, completely blocked the ability of Ang II to induce proliferation of cultured splenic lymphocytes. However, the mechanism underlying the beneficial actions of RAS inhibitors in preventing immune system injury has not been completely elucidated.

ARBs have been approved for use in treating hypertension, and this clinical practice has spread to many countries. In the present study, we demonstrate that ARBs have additional properties of suppressing antigen-specific Th1 responses in vivo. We evaluated olmesartan for its ability to ameliorate arthritis in the murine collagen-induced arthritis (CIA) model, which is an experimental animal model for human RA. To our knowledge, this is the first study to show antigen-specific immunosuppressive effects of the Th1 response of ARBs in vivo and to demonstrate the protective effects of ARBs in an arthritis model. Our findings suggest that ARBs may be a beneficial treatment for patients with RA.

MATERIALS AND METHODS

Mice. Female BALB/c mice (7 weeks of age) and male DBA/1 mice (6–7 weeks of age) were purchased from Japan SLC (Shizuoka, Japan). All of the animal experiments performed in this study were approved by the Animal Research Ethics Board of the Department of Allergy and Rheumatology at the University of Tokyo. The animals were maintained under specific pathogen-free conditions.

Immunization with ovalbumin (OVA) or bovine type II collagen (CII). OVA (grade V; Sigma, St. Louis, MO) or bovine CII (Chondrex, Seattle, WA) was solubilized to a concentration of 2 mg/ml in 0.05*M* acetic acid at 4°C, with constant overnight mixing. Mice were immunized in the footpads by subcutaneous injection of OVA or CII in Freund's complete adjuvant (CFA) emulsion (1 mg/ml; 0.1 ml/mouse). In some experiments, mice were immunized intraperitoneally with 2 μg/ml of OVA in 2 mg of aluminum hydroxide (alum). Immunizations were performed on day 0 and day 10.

Administration of ARBs. Olmesartan medoxomil (the prodrug of olmesartan), candesartan cilexetil, and telmisartan were kindly provided by Sankyo (Tokyo, Japan), Takeda Chemical Industries (Osaka, Japan), and Boehringer Ingelheim (Ingelheim, Germany), respectively. Olmesartan (10 or 15 mg/kg body weight), candesartan (10 mg/kg body weight), or telmisartan (10 mg/kg body weight) was administered orally in 0.5-ml suspensions every day or every other day, depending on the experiment, using a 2.25-mm feeding needle. In order to make uniform suspensions, olmesartan was suspended in carboxylmethyl cellulose sodium (CMC; Sigma), candesartan was suspended in methyl cellulose (Wako, Osaka, Japan), and telmisartan was suspended in hydroxyethyl cellulose (Roche Laboratories, Basel, Switzerland).

Cytokine analysis. Popliteal lymph node cells or splenocytes were isolated from the mice that had received olmesartan, candesartan, telmisartan, or vehicle only. After preparation of a single-cell suspension and red blood cell lysis, the cells were washed in Hanks' balanced salt solution (Sigma) and resuspended in X-VIVO 20 serum-free medium (Cambrex, Walkersville, MD). The cells were cultured in 96-well culture plates (Becton Dickinson, Franklin Lakes, NJ) at a concentration of 4×10^6 cells/ml with 3, 10, 30, 100, or 300 μg/ml of OVA or CII and medium (X-VIVO 20) alone. The cells were incubated at 37°C in a humidified atmosphere containing 5% CO_2. After 48 hours of incubation, the culture supernatants were collected, and the levels of IL-4, IL-10, and IFNγ were measured. These cytokines were determined by enzyme-linked immunosorbent assay (ELISA) using paired antibodies (PharMingen, San Diego, CA) for the corresponding cytokines, according to the manufacturer's protocol.

Proliferation assays. For the lymphocyte proliferation assay, popliteal lymph node cells or splenocytes were cultured in 96-well culture plates at a concentration of $3–4 \times 10^6$ cells/ml with 3, 10, 30, 100, or 300 μg/ml of OVA, 10 or 100 μg/ml of denatured CII, or medium (X-VIVO 20) alone. The cells were incubated at 37°C in a humidified atmosphere containing 5% CO_2. After 72 hours of culture, 1 μCi of ^{3}H-thymidine was added to each well, and the cells were incubated for an additional 16 hours at 37°C. After culturing, ^{3}H-thymidine uptake was detected using a microplate scintillation counter. Results are expressed as the mean ± SEM results of triplicate assays.

ELISA. For the measurement of OVA-specific IgG2a, IgG1, and IgE, blood samples were obtained from the inferior vena cava with a 25-gauge needle on day 7 and day 18 after the OVA/CFA immunization. After the samples had fully coagulated, they were centrifuged, and the sera were collected and stored at −80°C until used. Levels of OVA-specific IgG2a, IgG1, and IgE were determined by ELISA using biotinylated anti-mouse IgG2a, IgG1, and IgE antibodies for capture and biotinylated goat anti-mouse IgG2a, IgG1, and IgE antibodies for detection. For the measurement of CII-specific IgG1 and IgG2a, serum was collected on day 88, as described above.

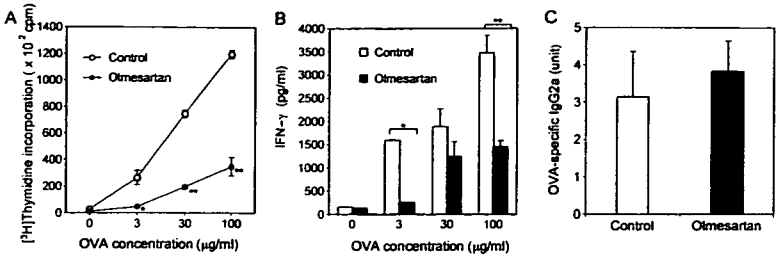

Figure 1. Olmesartan suppresses antigen-specific Th1 responses in BALB/c mice. BALB/c mice were immunized with ovalbumin (OVA) in Freund's complete adjuvant (CFA). Olmesartan (15 mg/kg body weight) or vehicle only (control) was administered every other day, beginning 5 days before immunization. Seven days after immunization, popliteal lymph node cells were obtained and cultured with OVA. **A,** After 72 hours of culture, ^{3}H-thymidine was added, and ^{3}H-thymidine incorporation was measured 16 hours later. * = $P < 0.05$ versus control; ** = $P < 0.0005$ versus control. **B,** After 48 hours of culture, supernatants were tested for interferon-γ (IFNγ) concentration by enzyme-linked immunosorbent assay (ELISA). * = $P < 0.05$; ** = $P < 0.001$. **C,** Seven days after mice were immunized with OVA in CFA, blood samples were obtained from the inferior vena cava. The levels of OVA-specific IgG2a were determined by ELISA. Values are the mean ± SEM.

Induction of CIA. CII (Chondrex) was solubilized to a concentration of 2 mg/ml in 0.05*M* acetic acid at 4°C, with constant overnight mixing. For the induction of CIA, CII was emulsified with an equal volume (1:1) of CFA (4 mg/ml; Chondrex). Mice were injected subcutaneously ~1–2 cm from the base of the tail with 100 μl of the emulsion (day 0). On day 21, the mice received a booster injection, for which the collagen was emulsified with Freund's incomplete adjuvant (IFA; Difco, Detroit, MI) instead of CFA; the mice were injected with 100 μl of the emulsion near the base of the tail at a location different from that used for the first injection. Development of arthritis was assessed by inspection 3 times weekly. The clinical severity of arthritis in each paw was quantified according to a graded scale from 0 to 4, as follows: 0 = no swelling, 1 = swelling in one digit or mild edema, 2 = moderate swelling affecting several digits, 3 = severe swelling affecting most digits, and 4 = the most severe swelling and/or ankylosis. A mean arthritis score was determined by summing the scores of all joints of all mice and dividing the result by the total number of mice in the group. The mean ± SEM values were determined.

Histopathology. All mice were killed on day 74, and the joints of the left hind paw were fixed in 10% phosphate buffered formaldehyde solution and decalcified in Parengy decalcification solution overnight. The tissue was then processed and embedded in paraffin. Tissue sections were stained with hematoxylin and eosin (H&E), using standard methodology. The joints were studied by 2 blinded examiners from the Sapporo General Pathology Institute (Sapporo, Japan). The pathologic condition was scored in 5 categories, as follows: cartilage, cellularity, pannus, bone erosion, and ankylosis. Each category was graded from 0 to 4 as follows: 0 = normal, 1 = minimal, 2 = mild, 3 = moderate, and 4 = marked.

Statistical analysis. Results are expressed as the mean ± SEM. The Mann-Whitney U test was used to analyze the clinical scores, the incidence of severe arthritis, and histologic findings. The unpaired *t*-test was used to analyze the results of cytokine and proliferation assays and serum antibody levels. *P* values less than 0.05 were considered significant.

RESULTS

Suppression of OVA-specific Th1 response by ARBs. To examine the immunomodulatory effects of ARBs, we administered olmesartan in vivo and checked OVA-specific T cell proliferation and cytokine production following immunization with OVA. BALB/c mice received either olmesartan (15 mg/kg) suspended in CMC or CMC only, every day beginning 5 days before immunization until the day on which the mice were killed. Seven days after immunization, we obtained blood samples and popliteal lymph nodes from the mice and performed cytokine analyses and proliferation assays. As shown in Figure 1A, in the mice that received olmesartan, OVA-specific proliferation was significantly suppressed compared with that in the control group. IFNγ production (Figure 1B) was also reduced in the olmesartan-treated mice. In contrast, no production of either IL-4 or IL-10 was detected in either group (results not shown). Furthermore, there were no significant differences between groups in the serum levels of OVA-specific IgG2a (Figure 1C).

To examine whether the immunosuppressive effect of Th1 is olmesartan-specific, we examined the effects of the 2 other ARBs, candesartan and telmisartan, using the same method. In the candesartan-treated

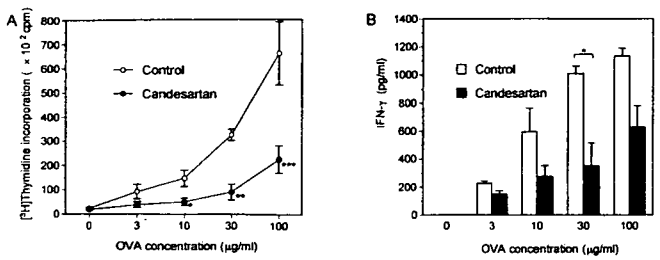

Figure 2. Candesartan reduces OVA-specific Th1 responses in vivo. BALB/c mice were immunized with OVA in CFA. Either candesartan (10 mg/kg) suspended in methylcellulose or methylcellulose only (control) was administered every day, beginning 5 days before immunization. The mice were killed, and the popliteal lymph node cells were cultured as described in Figure 1. **A,** OVA-specific proliferation of the lymphocytes was measured by ^{3}H-thymidine incorporation. * = $P <$ 0.05 versus control; ** = $P < 0.005$ versus control; *** = $P < 0.01$ versus control. **B,** Production of IFNγ was measured by ELISA. * = $P < 0.05$. Values are the mean ± SEM. See Figure 1 for definitions.

group, proliferation and IFNγ production (Figures 2A and B) were suppressed significantly, to the same extent as in the olmesartan-treated group ($P < 0.005$ to $P <$ 0.05). In the telmisartan-treated group, proliferation and IFNγ production were also reduced compared with that in the control group, but the immune suppression of the Th1 response was milder than that observed with the other ARBs (results not shown). Serum levels of OVA-specific IgG2a also were not significantly different between the control and the telmisartan-treated groups (results not shown). These results suggested that ARBs suppress OVA-specific Th1 responses in vivo.

Suppression of CII-specific Th1 response by ARBs. To confirm that the immunosuppressive effect of ARBs is antigen-specific, we examined whether olmesartan suppressed the response to CII or mitogen after immunization with CII in CFA. DBA/1 mice received olmesartan, 10 mg/kg, every day beginning 5 days before being immunized with CII in CFA. Nine days after immunization, we obtained blood samples and popliteal lymph nodes from the mice. The lymphocytes were cultured with CII or concanavalin A in vitro, and cytokine analyses and proliferation assays were carried out. As shown in Figures 3A and B, CII-specific proliferation was significantly suppressed in the olmesartan-treated group, in which IFNγ production was also suppressed. Th2 cytokines, such as IL-4 and IL-10, were not detected (results not shown). Moreover, there were no statistically significant differences between the serum levels of CII-specific IgG1 and IgG2a (results not shown). These results suggested that olmesartan influenced only the antigen-specific response in vivo, because concanavalin A–induced proliferation and production of IFNγ were not affected (Figures 3A and B).

Suppression of OVA-specific Th2 cell proliferation by ARBs. We also studied the influence of olmesartan on Th2 responses. BALB/c mice received intraperitoneal injections of OVA/alum on day 0 and day 10. Beginning on day −9 until the day on which the mice were killed, the mice received either olmesartan (10 mg/kg) suspended in CMC or CMC only (control) every other day. On day 18, splenocytes were obtained, and cytokine production and proliferation were analyzed. At the same time, OVA-specific IgG1 and IgE levels in sera were measured. As shown in Figure 4, proliferative responses of spleen cells isolated from olmesartan-

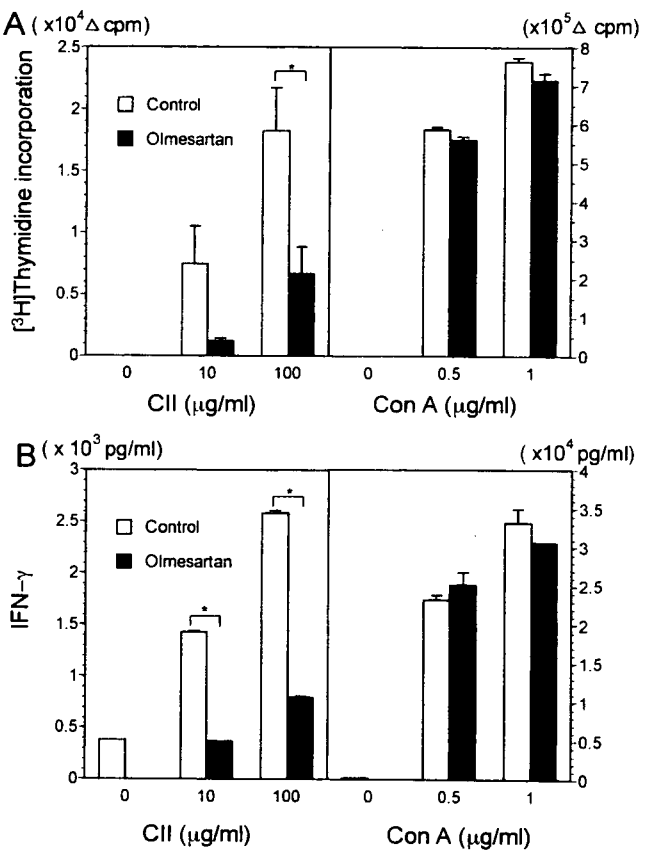

Figure 3. Administration of olmesartan to DBA/1 mice inhibits the Th1 response induced by immunization with type II collagen (CII) in CFA. Beginning 5 days before immunization, olmesartan (10 mg/kg) or vehicle only (control) was administered every day until the mice were killed. On day 9, popliteal lymph node cells were obtained and cultured with CII (10 μg/ml or 100 μg/ml), concanavalin A (Con A; 0.5 μg/ml or 1.0 μg/ml), or medium alone. **A,** Proliferation of lymphocytes was measured by ^{3}H-thymidine incorporation. * = $P < 0.05$. **B,** Production of IFNγ was measured by ELISA. * = $P < 0.0005$. Values are the mean and SEM. See Figure 1 for other definitions.

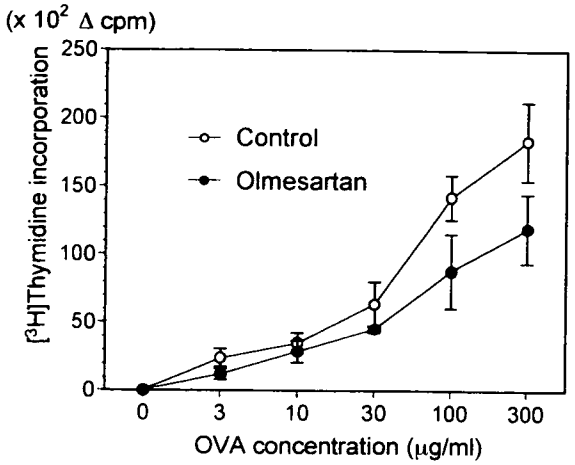

Figure 4. Olmesartan suppresses ovalbumin (OVA)-specific Th2 proliferation. BALB/c mice were immunized intraperitoneally with 2 μg of OVA in 2 mg of aluminum hydroxide on days 0 and 10. Beginning 9 days before immunization, olmesartan (10 mg/kg) suspended in carboxylmethyl cellulose sodium (CMC) or CMC only (control) was administered every day until the mice were killed. On day 18, spleen cells and blood samples were obtained. Spleen cells were cultured with OVA or medium alone. Proliferation of the cells was measured by the method described in Figure 1. Values are the mean ± SEM.

treated mice were lower than those of cells isolated from controls, but the differences between groups were not statistically significant. Serum OVA-specific IgG1 and IgE levels were not statistically significantly different between the olmesartan-treated group and the control group (results not shown). Concentrations of IL-4, IL-10, and IFNγ in the culture supernatants were below the detection limit of the ELISA (data not shown). These results suggested that although the suppression level of the Th2 response was considerably weaker than that of the Th1 response, ARBs reduced OVA-specific proliferation of Th2 cells without shifting from the Th1 response to the Th2 response.

Blockade of the development and progression of CIA by ARBs. CIA is a commonly used mouse model of human RA. Because CII-specific immune responses by draining lymph node cells were suppressed in vitro (Figure 3), we next administered olmesartan to mice with CIA in order to examine immunosuppression of Th1 responses by ARBs in this disease model. Mice received immunizations with CII in CFA on day 0 and with CII in IFA on day 21. Beginning on day −9, each mouse received olmesartan (10 mg/kg) suspended in CMC or CMC only (control); administration continued every other day until day 70. The severity of arthritis in the mice was scored on a scale of 0–4 for each limb. The mean arthritis score was determined by summing the scores of all joints of the mice and dividing the resulting value by the total number of mice in the group. The incidence of severe arthritis was determined by the percentage of mice that had at least 1 joint with a score of 4. Progression of arthritis was evaluated until day 70 after immunization, and the number of paws affected and the mean clinical scores were recorded.

In the control group, severe arthritis began to appear beginning ~35 days after immunization and peaked on day 70 after immunization (Figure 5A). Olmesartan-treated mice had milder arthritis compared with control mice (mean ± SEM arthritis score 10.9 ± 0.57 versus 13.9 ± 1.0), and their scores were statistically significantly lower than those of controls on days 51, 56, 66, and 70 as well as at the end of the experiment (Figure 5A). Thirty-nine days after immunization, the incidence of arthritis was 100% in both the control and olmesartan-treated groups, and this incidence remained unchanged for the rest of the experiment (Figure 5B). The incidence of severe arthritis (defined as a score of 4) was lower in the olmesartan-treated group than in the control group treated with CMC alone (Figure 5C), but there was no statistically significant difference between these groups.

To determine whether olmesartan administration prevented articular destruction, histologic sections obtained from the hind paws of the mice were examined. The left hind paws of all mice in each group (n = 10 per group) were analyzed grossly and histopathologically by staining with H&E on day 74 after immunization. The histopathologic arthritis score was assessed according to findings of cartilage destruction, synovial hypertrophy, pannus formation, bone erosion, and ankylosis. Results of the histopathologic examinations are summarized in Table 1. Histopathology revealed statistically significant reductions in cartilage loss, cellular infiltrates, pannus formation, bone erosion, and ankylosis. Thus, suppression of the clinical scores correlated with the reduction in histopathologic findings. These results suggest that ARBs blocked the development and progression of CIA by suppressing Th1 responses to CII and local inflammation.

It was important to determine whether similar effects can be obtained by administering olmesartan after the onset of CIA. Therefore, we next administered olmesartan to DBA/1 mice before and after CIA became clinically detectable. For this experiment, olmesartan was administered every day. According to the prophylactic protocol, olmesartan (10 mg/kg) or vehicle only was administered, beginning 5 days before immunization

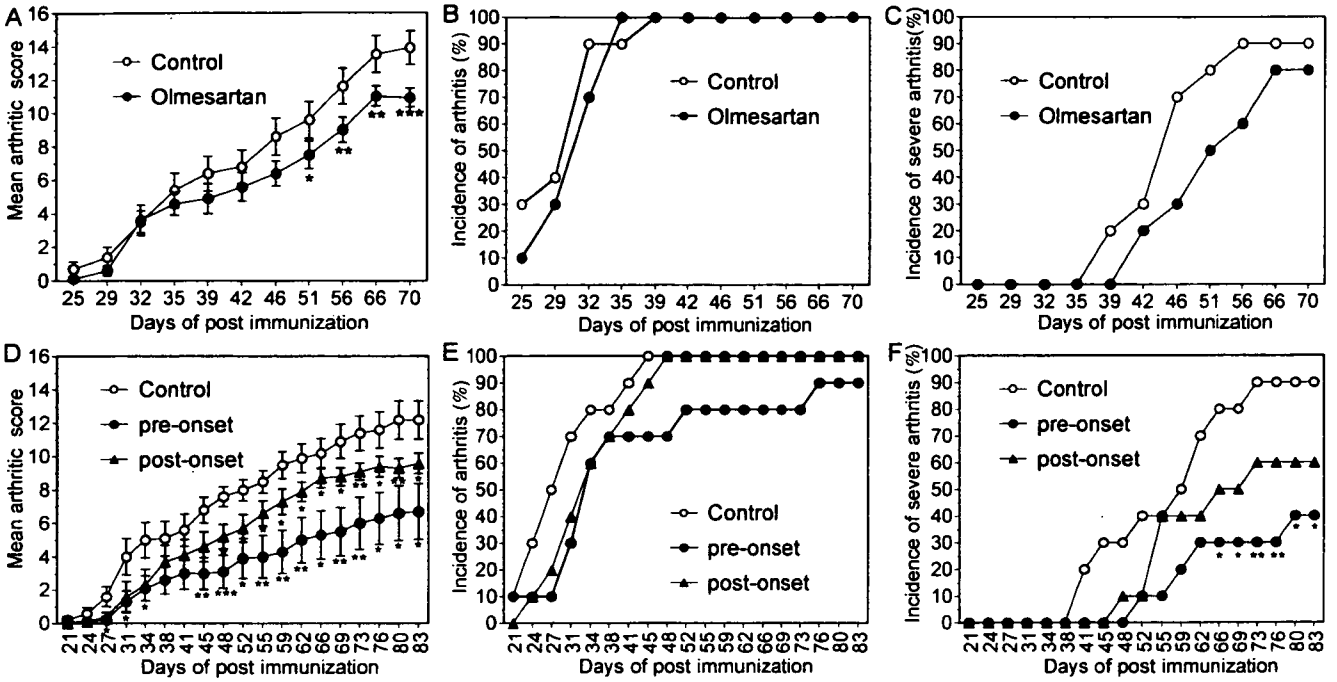

Figure 5. Administration of olmesartan blocks development of collagen-induced arthritis (CIA). Arthritis was induced in DBA/1 mice by immunization with type II collagen (CII) in Freund's complete adjuvant on day 0. On day 21, mice were injected subcutaneously with CII in Freund's incomplete adjuvant. **A–C,** Administration of olmesartan before immunization. Beginning 9 days before immunization and continuing until day 70, mice received olmesartan (10 mg/kg) suspended in carboxylmethyl cellulose sodium (CMC) or CMC only (control) every other day. Clinical scores were determined as described in Materials and Methods. **A,** Mean ± SEM arthritis scores in the 2 groups. * = $P < 0.05$ versus control; ** = $P < 0.01$ versus control; *** = $P < 0.005$ versus control. **B,** Incidence of arthritis in the 2 groups. **C,** Percentage of mice with severe arthritis (arthritis score = 4). Representative results of 2 independent experiments are shown (n = 10 mice/group). **D–F,** Administration of olmesartan after disease onset. Mice received olmesartan (10 mg/kg) every day, beginning on the day after clinically evident onset of arthritis and continuing until day 87 after onset. **D,** Mean ± SEM arthritis scores in mice that received CMC alone (control; n = 10), mice that received olmesartan 5 days before immunization (pre-onset; n = 10), and mice that received olmesartan beginning on the day after onset of clinically evident arthritis (post-onset; n = 10). * = $P < 0.05$ versus control; ** = $P < 0.01$ versus control; *** = $P < 0.005$ versus control. **E,** Incidence of arthritis. **F,** Percentage of mice with severe arthritis (arthritis score = 4). * = $P < 0.05$ versus control; ** = $P < 0.01$ versus control.

and continuing until day 87; according to the therapeutic protocol, olmesartan (10 mg/kg) or vehicle only was administered, beginning on day 25 and continuing until day 87 (Figures 5D–F).

Control mice that were treated with vehicle only according to the prophylactic protocol showed signs of arthritis beginning ~21 days after immunization and peaking on day 80 after immunization (Figure 5D). Compared with daily administration of CMC only, administration of olmesartan according to the prophylactic protocol effectively suppressed disease. Among mice treated according to the prophylactic protocol, the mean ± SEM arthritis score at the end of the experiment was 12.2 ± 1.14 in the control group versus 6.7 ± 1.69 ($P = 0.029$) in the olmesartan-treated group (Figure 5D). In contrast, among mice treated with olmesartan according to the therapeutic protocol, the mean ± SEM arthritis score at the end of the experiment was 9.6 ± 0.62 ($P = 0.014$) (Figure 5D). Among mice treated according to the prophylactic protocol, the mean arthritis score (Figure 5D), incidence of arthritis (Figure 5E), and incidence of severe arthritis (Figure 5F) in the olmesartan-treated group were suppressed compared

Table 1. Impact of ARB treatment in the murine CIA model*

Pathology category	Control	ARB-treated	P†
Cartilage	2.9 ± 1.20	1.0 ± 1.41	0.008
Cellularity	2.9 ± 1.20	1.0 ± 1.33	0.006
Pannus	2.7 ± 1.25	1.1 ± 1.52	0.028
Bone erosion	2.9 ± 1.20	0.9 ± 1.20	0.003
Ankylosis	2.6 ± 1.0	1.0 ± 1.33	0.013

* Values are the mean ± SEM pathology score (0 = normal, 1 = minimal, 2 = mild, 3 = moderate, 4 = marked). ARB = angiotinsin II receptor blocker; CIA = collagen-induced arthritis.
† By Mann-Whitney U test.

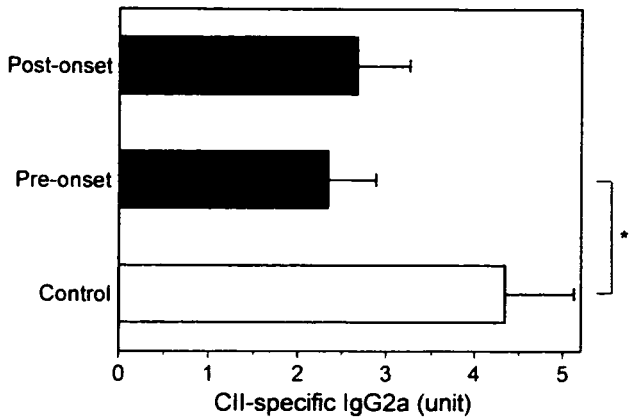

Figure 6. Measurement of type II collagen (CII)–specific IgG2a. In the experiment referred to in Figure 5D, blood samples were obtained from the inferior vena cava on day 88. Levels of anti-CII IgG2a in the 3 groups (control, pre-onset, and post-onset [n = 10 per group]) were determined by enzyme-linked immunosorbent assay. Values are the mean and SEM. * = $P < 0.05$.

with the control group. Among mice treated according to the therapeutic protocol, the incidence of severe arthritis was reduced compared with that in the control group (Figure 5F), but 48 days after immunization the incidence of arthritis was 100% in both the control and olmesartan-treated mice and remained unchanged for the duration of the experiment (Figure 5E). Finally, on day 88 after immunization, serum CII-specific levels of IgG1 and IgG2a were reduced in the olmesartan-treated group (Figure 6), and the reduction in CII-specific IgG2a levels was significant ($P = 0.049$). These data indicated that olmesartan suppressed CIA both before and after disease onset.

DISCUSSION

In this study, we examined the influence of ARBs on antigen-specific Th1 and Th2 responses in vivo. Furthermore, we assessed the immunosuppressive effects of ARBs on the development of the murine CIA model, which is a Th1-driven animal model of human RA. Naive CD4+ T cells differentiate into 2 distinct subpopulations, Th1 cells and Th2 cells, each of which produces its own panel of cytokines and mediates separate functions (16). Th1 cells secrete IFNγ, IL-2, and tumor necrosis factor α (16), thereby activating macrophages, inducing delayed-type hypersensitivity responses, and helping in the immunoglobulin isotype switch from IgM to IgG2a (17). In contrast, Th2 cells secrete IL-4, IL-5, and IL-10 in response to extracellular bacterial pathogens and help in the immunoglobulin isotype switch from IgM to IgG1 and IgE (16,17).

In our study, the proliferation of antigen-specific Th1 cells and the production of IFNγ in vitro were suppressed by ARB administration in vivo (Figures 1 and 2), although the suppressive effect of telmisartan was smaller than that of the other ARBs, olmesartan and candesartan (data not shown). However, production of the Th1-dependent IgG antibody (IgG2a) was not suppressed (Figure 1C). In addition, ARBs also reduced antigen-specific Th2 cell proliferation, although the level of suppression of Th2 responses was lower than that of Th1 responses (Figure 4). As in the case of Th1, production of Th2-dependent IgG antibody (IgG1) was not significantly different between ARB-treated mice and controls (data not shown). Generally, the proliferation of Th1 cells prevents the generation of Th2 cells, whereas the proliferation of Th2 cells prevents the generation of Th1 cells (18). In a continuous Ang II infusion model of rats, Shao et al (5) showed that Ang II polarized CD4+ T cells into Th1 lymphocytes, and that the polarization was normalized by ARBs. Interestingly, in our study ARBs suppressed not only Th1 responses but also Th2 responses in vivo without enhancing the production of Th2 or Th1 cytokines. It is possible that ARBs suppress both Th1 and Th2 responses in cases in which CD4+ T cells are extremely polarized into Th1 or Th2 cells.

Several recent studies have demonstrated the protective effects of RAS antagonists in immunologically mediated conditions such as myocarditis, chronic allograft rejection, and antiglomerular basement membrane nephritis (9–12,14,19–21). However, the mechanism underlying the beneficial actions of RAS inhibitors in preventing immunologic injury in these models is still unclear. To analyze the immunosuppressive effect of ARBs on Th1 responses in a disease model, we administered olmesartan orally in a murine CIA model. We chose olmesartan from among the ARBs because it suppressed Th1 responses in vivo more potently than did the other ARBs tested. There were no signs that blood pressure was reduced in any of the mice throughout this study. In our study, the development and progression of CIA appeared to be blocked in the olmesartan-treated group (Figure 5). Furthermore, not only the clinical scores but also results of the histologic analysis of olmesartan-treated mice revealed that their joints had much milder inflammation compared with control mice (Table 1). Importantly, olmesartan was effective even when it was introduced after the onset of arthritis (Figures 5D–F). These data suggest that ARBs may be

useful therapeutically in RA, and that Ang II may be involved in the development of CIA.

CIA is associated with a Th1-polarized immune response, rendering it an excellent model in which to explore the effect of olmesartan in vivo. To confirm the relationship between the CII-specific immune responses in vitro and CIA in vivo, we examined CII-specific proliferation and cytokine production by draining lymph node cells obtained from mice belonging to the same strain, DBA/1 (Figure 3). According to our data, CII-specific proliferation and IFNγ production were suppressed in vitro (Figures 3A and B). Moreover, in order to make sure that the suppressive effects of olmesartan were antigen-specific, we examined the response of lymphocytes to a mitogen (Figures 3A and B). Concanavalin A–induced proliferation and IFNγ production were similar between the olmesartan-treated and control groups, indicating that olmesartan suppresses only antigen-specific responses. During the acute phase (day 9), the levels of CII-specific IgG2a were also similar between the olmesartan and control groups, but during a later phase (day 88) the levels in the olmesartan group were significantly suppressed (Figure 6). These data suggest that olmesartan can effectively suppress anti-collagen B cell responses during a later phase of CIA.

It has been reported that immunocompetent cells, including T cells, macrophages, and dendritic cells, are equipped with components of the RAS, and that they can participate in the production of Ang II (22–24). It has also been reported that AT_1 receptors are expressed in human synovium (25), and that ACE activity in synovial fluid is increased in patients with arthritis (26–28). It has been demonstrated that both AT_1 and AT_2 receptors activate the NF-κB pathway and up-regulate the NF-κB gene (6–8,29–32). The constitutive activation of the NF-κB pathway is often associated with inflammatory diseases such as RA, inflammatory bowel diseases, multiple sclerosis, and asthma (33). In our study, ARB administration attenuated the development of CIA clinically and pathologically, suggesting that Ang II, which in the CIA model is locally generated in the synovium, exacerbates inflammation of the synovium in articular muscle via the up-regulation of NF-κB. Alternatively, it has been speculated that another mechanism allows ARBs to directly suppress Th1 responses, because the AT_1 receptor is present on T cells (34–36).

Ang II acts via AT_1 and/or AT_2 receptors. AT_1 receptors are involved in cell proliferation as well as in the production of cytokines and extracellular matrix proteins by cultured cells (4,32,37,38). AT_2 receptors regulate blood pressure control and renal natriuresis, and, after vascular injury, inhibit both cell proliferation and neointimal formation. Because Ang II activates NF-κB via both AT_1 and AT_2 receptors, and because Esteban et al (31) showed that only combined treatment with AT_1 and AT_2 antagonists completely blocked renal inflammatory infiltration and NF-κB activation in Ang II–infused mice, therapy combining AT_1 and AT_2 antagonists may be more effective than therapy using AT_1 antagonist alone in reducing the inflammation of arthritis. In this study, we administered a relatively high dose of olmesartan to mice. This approach was used because Shao et al demonstrated an increase in the level of IFNγ and a decrease in the level of IL-4 in Ang II–infused rats and showed that this imbalance in T cell subsets was reversed by olmesartan, in a dose-dependent manner (5). Furthermore, in the CIA model, mean arthritis scores were only slightly improved when olmesartan was administered every other day but were extremely improved when olmesartan was administered daily. Thus, for more effective suppression, the means of administration and the doses of ARB need to be modified.

In conclusion, our findings suggest that ARBs restrain exacerbation of arthritis in the CIA model. It was previously reported that the ACE inhibitor captopril improved arthritis symptoms and laboratory values in patients with active arthritis (13). However, it has never been reported that ARBs may be of therapeutic benefit to patients with arthritis. It has become clear that several serine proteases, including kallikrein, cathepsin G, and chymase, are related to ACE-independent Ang II formation in vivo (39,40); in particular, chymase is responsible for most Ang II formation in humans (41). The ARBs have much greater potential than ACE inhibitors for blocking angiotensin II production, and they may be better drugs for patients with arthritis and hypertension.

REFERENCES

1. Matsubara H. Pathophysiological role of angiotensin II type 2 receptor in cardiovascular and renal diseases. Circ Res 1998;83: 1182–91.
2. De Gasparo M, Catt KJ, Inagami T, Wright JW, Unger T. International union of pharmacology. XXIII. The angiotensin II receptors. Pharmacol Rev 2000;52:415–72.
3. Griendling KK, Lassegue B, Alexander RW. Angiotensin receptors and their therapeutic implications. Annu Rev Pharmacol Toxicol 1996;36:281–306.
4. Timmermans PB, Wong PC, Chiu AT, Herblin WF, Benfield P, Carini DJ, et al. Angiotensin II receptors and angiotensin II receptor antagonists. Pharmacol Rev 1993;45:205–51.
5. Shao J, Nangaku M, Miyata T, Inagi R, Yamada K, Kurokawa K, et al. Imbalance of T-cell subsets in angiotensin II-infused hypertensive rats with kidney injury. Hypertension 2003;42:31–8.
6. Ruiz-Ortega M, Lorenzo O, Ruperez M, Suzuki Y, Egido J. Angiotensin II activates nuclear transcription factor-κB in aorta of

normal rats and in vascular smooth muscle cells of AT1 knockout mice. Nephrol Dial Transplant 2001;16 Suppl 1:27–33.
7. Ruiz-Ortega M, Lorenzo O, Ruperez M, Konig S, Wittig B, Egido J. Angiotensin II activates nuclear transcription factor κB through AT(1) and AT(2) in vascular smooth muscle cells: molecular mechanisms. Circ Res 2000;86:1266–72.
8. Ruiz-Ortega M, Lorenzo O, Ruperez M, Blanco J, Egido J. Systemic infusion of angiotensin II into normal rats activates nuclear factor-κB and AP-1 in the kidney: role of AT(1) and AT(2) receptors. Am J Pathol 2001;158:1743–56.
9. Amuchastegui SC, Azzollini N, Mister M, Pezzotta A, Perico N, Remuzzi G. Chronic allograft nephropathy in the rat is improved by angiotensin II receptor blockade but not by calcium channel antagonism. J Am Soc Nephrol 1998;9:1948–55.
10. Benediktsson H, Chea R, Davidoff A, Paul LC. Antihypertensive drug treatment in chronic renal allograft rejection in the rat: effect on structure and function. Transplantation 1996;62:1634–42.
11. Mackenzie HS, Ziai F, Nagano H, Azuma H, Troy JL, Rennke HG, et al. Candesartan cilexetil reduces chronic renal allograft injury in Fisher-Lewis rats. J Hypertens Suppl 1997;15:S21–5.
12. Furukawa Y, Matsumori A, Hirozane T, Sasayama S. Angiotensin II receptor antagonist TCV-116 reduces graft coronary artery disease and preserves graft status in a murine model: a comparative study with captopril. Circulation 1996;93:333–9.
13. Martin MF, Surrall KE, McKenna F, Dixon JS, Bird HA, Wright V. Captopril: a new treatment for rheumatoid arthritis? Lancet 1984;1:1325–8.
14. Godsel LM, Leon JS, Wang K, Fornek JL, Molteni A, Engman DM. Captopril prevents experimental autoimmune myocarditis. J Immunol 2003;171:346–52.
15. Nataraj C, Oliverio MI, Mannon RB, Mannon PJ, Audoly LP, Amuchastegui CS, et al. Angiotensin II regulates cellular immune responses through a calcineurin-dependent pathway. J Clin Invest 1999;104:1693–701.
16. Mosmann TR, Coffman RL. TH1 and TH2 cells: different patterns of lymphokine secretion lead to different functional properties. Annu Rev Immunol 1989;7:145–73.
17. Finkelman FD, Goroff DK, Fultz M, Morris SC, Holmes JM, Mond JJ. Polyclonal activation of the murine immune system by an antibody to IgD. X. Evidence that the precursors of IgG1-secreting cells are newly generated membrane IgD+ B cells rather than the B cells that are initially activated by anti-IgD antibody. J Immunol 1990;145:3562–9.
18. Paul WE, Seder RA. Lymphocyte responses and cytokines. Cell 1994;76:241–51.
19. Tanaka A, Matsumori A, Wang W, Sasayama S. An angiotensin II receptor antagonist reduces myocardial damage in an animal model of myocarditis. Circulation 1994;90:2051–5.
20. Hisada Y, Sugaya T, Yamanouchi M, Uchida H, Fujimura H, Sakurai H, et al. Angiotensin II plays a pathogenic role in immune-mediated renal injury in mice. J Clin Invest 1999;103: 627–35.
21. Leon JS, Wang K, Engman DM. Captopril ameliorates myocarditis in acute experimental Chagas disease. Circulation 2003;107: 2264–9.
22. Suzuki Y, Ruiz-Ortega M, Lorenzo O, Ruperez M, Esteban V, Egido J. Inflammation and angiotensin II. Int J Biochem Cell Biol 2003;35:881–900.
23. Nahmod KA, Vermeulen ME, Raiden S, Salamone G, Gamberale R, Fernandez-Calotti P, et al. Control of dendritic cell differentiation by angiotensin II. FASEB J 2003;17:491–3.
24. Rodriguez-Iturbe B, Pons H, Herrera-Acosta J, Johnson RJ. Role of immunocompetent cells in nonimmune renal diseases. Kidney Int 2001;59:1626–40.
25. Walsh DA, Suzuki T, Knock GA, Blake DR, Polak JM, Wharton J. AT1 receptor characteristics of angiotensin analogue binding in human synovium. Br J Pharmacol 1994;112:435–42.
26. Walsh DA, Catravas J, Wharton J. Angiotensin converting enzyme in human synovium: increased stromal [(125)I]351A binding in rheumatoid arthritis. Ann Rheum Dis 2000;59:125–31.
27. Veale D, Yanni G, Bresnihan B, FitzGerald O. Production of angiotensin converting enzyme by rheumatoid synovial membrane. Ann Rheum Dis 1992;51:476–80.
28. Lowe JR, Dixon JS, Guthrie JA, McWhinney P. Serum and synovial fluid levels of angiotensin converting enzyme in polyarthritis. Ann Rheum Dis 1986;45:921–4.
29. Lorenzo O, Ruiz-Ortega M, Suzuki Y, Ruperez M, Esteban V, Sugaya T, et al. Angiotensin III activates nuclear transcription factor-κB in cultured mesangial cells mainly via AT(2) receptors: studies with AT(1) receptor-knockout mice. J Am Soc Nephrol 2002;13:1162–71.
30. Wolf G, Wenzel U, Burns KD, Harris RC, Stahl RA, Thaiss F. Angiotensin II activates nuclear transcription factor-κB through AT1 and AT2 receptors. Kidney Int 2002;61:1986–95.
31. Esteban V, Ruperez M, Vita JR, Lopez ES, Mezzano S, Plaza JJ, et al. Effect of simultaneous blockade of AT1 and AT2 receptors on the NFκB pathway and renal inflammatory response. Kidney Int Suppl 2003;86:S33–8.
32. Sadoshima J. Cytokine actions of angiotensin II. Circ Res 2000; 86:1187–9.
33. Li Q, Verma IM. NF-κB regulation in the immune system. Nat Rev Immunol 2002;2:725–34.
34. Tsutsumi K, Stromberg C, Saavedra JM. Characterization of angiotensin II receptor subtypes in the rat spleen. Peptides 1992;13:291–6.
35. Shimada K, Yazaki Y. Binding sites for angiotensin II in human mononuclear leucocytes. J Biochem (Tokyo) 1978;84:1013–5.
36. Gomez RA, Norling LL, Wilfong N, Isakson P, Lynch KR, Hock R, et al. Leukocytes synthesize angiotensinogen. Hypertension 1993;21:470–5.
37. Egido J. Vasoactive hormones and renal sclerosis. Kidney Int 1996;49:578–97.
38. Wolf G, Neilson EG. Angiotensin II as a renal growth factor. J Am Soc Nephrol 1993;3:1531–40.
39. Takai S, Shiota N, Kobayashi S, Matsumura E, Miyazaki M. Induction of chymase that forms angiotensin II in the monkey atherosclerotic aorta. FEBS Lett 1997;412:86–90.
40. Takai S, Jin D, Sakaguchi M, Miyazaki M. Chymase-dependent angiotensin II formation in human vascular tissue. Circulation 1999;100:654–8.
41. Kokkonen JO, Saarinen J, Kovanen PT. Regulation of local angiotensin II formation in the human heart in the presence of interstitial fluid: inhibition of chymase by protease inhibitors of interstitial fluid and of angiotensin-converting enzyme by Ang-(1-9) formed by heart carboxypeptidase A-like activity. Circulation 1997;95:1455–63.